Molecular Pharmacology Fast Forward. Published on November 15, 2012 as doi:10.1124/mol.112.080879

CB_1 RECEPTOR ALLOSTERIC MODULATORS DISPLAY BOTH AGONIST AND SIGNALING PATHWAY SPECIFICITY

Gemma L. Baillie, James G. Horswill, Sharon Anavi-Goffer, Patricia H. Reggio, Daniele Bolognini, Mary E. Abood, Sean McAllister, Phillip G. Strange, Gary J. Stephens, Roger G. Pertwee & Ruth A. Ross.

School of Medical Sciences, Institute of Medical Sciences, University of Aberdeen, Aberdeen, AB25 2ZD UK (GLB,SAG,DB,RGP,RAR). Prosidion Limited, Windrush Court, Oxford, UK (JH). School of Pharmacy, University of Reading, Reading, UK (GJS,PGS). University of North Carolina, North Carolina, 27402. USA (PHR). Temple University, Philadelphia, PA19122, USA (MEA). Dept of Behavioral Sciences & Molecular Biology, Ariel University Center, Israel (SAG). Calif Pacific Med Center, Research Institute, San Francisco, CA 94107 USA (SMcA). Department of Pharmacology & Toxicology, Faculty of Medicine, University of Toronto, 1 King's College Circle, Toronto, Ontario, Canada M5S 1A8 (RAR).

Molecular Pharmacology Fast Forward. Published on November 15, 2012 as DOI: 10.1124/mol.112.080879
This article has not been copyedited and formatted. The final version may differ from this version.

RUNNING TITLE

Running Title: Cannabinoid CB1 allosteric modulators: signaling specificity

Authors for correspondence:
Current address: Ruth A. Ross, Department of Pharmacology & Toxicology, Faculty of Medicine, University of Toronto, 1 King's College Circle, Toronto, Ontario, Canada M5S 1A8. ruth.ross@utoronto.ca

Text pages
Tables: 6
Figures: 11
References: 28
Abstract: 248
Introduction: 747
Discussion: 2000

Abbreviations:

Bovine serum albumin, BSA; Cannabinoid, CB; Dimethyl sulphoxide, DMSO; ERK1/2, extracellular signal-regulated kinases 1/2; Guanine diphosphate, GDP; G protein-coupled receptor, GPCR; Guanine triphosphate, GTP; PTX, pertussis toxin.

Molecular Pharmacology Fast Forward. Published on November 15, 2012 as DOI: 10.1124/mol.112.080879
This article has not been copyedited and formatted. The final version may differ from this version.

Abstract

We have previously identified allosteric modulators of the cannabinoid CB_1 receptor (Org 27569, PSNCBAM-1) which display a contradictory pharmacological profile: increasing the specific binding of the CB_1 receptor agonist [^{3}H]CP55940 but producing a decrease in CB_1 receptor agonist efficacy. Here we investigated the effect one or both compounds in a broad range of signalling endpoints linked to CB_1 receptor activation. We assessed the effect of these compounds on CB_1 receptor agonist-induced [^{35}S]GTPγS binding, inhibition and stimulation of forskolin-stimulated cAMP production, phosphorylation of ERK, and β arrestin recruitment. We also investigated the effect of these allosteric modulators on CB_1 agonist binding kinetics. Both compounds display ligand dependence, being significantly more potent as modulators of CP55940 signalling as compared to WIN55212 and having little effect on [^{3}H]WIN55212 binding. Org 27569 displays biased antagonism whereby it *inhibits:* agonist-induced [^{35}S]GTPγS binding, simulation (Gαs mediated) and inhibition (Gαi mediated) of cAMP production and β arrestin recruitment. In contrast, it acts as an *enhancer* of agonist-induced ERK phosphoryation. Alone, the compound can act also as an *allosteric agonist*, increasing cAMP production and ERK phosphorylation. We find that in both saturation and kinetic binding experiments, the Org 27569 and PSNCBAM-1 appeared to influence only orthosteric ligand *maximum occupancy* rather than affinity. The data indicate that the allosteric modulators share a common mechanism whereby they increase available high affinity CB_1 agonist binding sites. The receptor conformation stabilised by the allosterics appears to induce signalling and also selectively traffics orthosteric agonist signalling via the ERK phosphorylation pathway.

Molecular Pharmacology Fast Forward. Published on November 15, 2012 as DOI: 10.1124/mol.112.080879
This article has not been copyedited and formatted. The final version may differ from this version.

Introduction

The endocannabinoid system encompasses a family of endogenous ligands, prominent examples including arachidonoylethanolamide (anandamide) and 2-arachidonoyl glycerol (2-AG), both of which are synthesised on demand and are rapidly hydrolysed by the enzymes. Within the brain, the distribution of CB_1 receptors is heterogeneous; they are found predominantly on nerve terminals where they attenuate neurotransmitter release. CB_1 receptor competitive antagonists/inverse agonists were developed for the treatment of obesity and nicotine addiction but were withdrawn due to associated serious psychiatric side-effects (Nathan et al., 2011).

In 2005 we identified the first allosteric modulators of the cannabinoid CB_1 receptor (Price et al., 2005; Ross, 2007), followed by a structurally-related compound, PSNCBAM-1 (Horswill et al., 2007). These compounds modulate electrically-evoked contractions in the mouse vas deferens (Price et al., 2005), affect CB_1 ligand modulation of synaptic transmission (Wang et al., 2011) and have hypophagic effects *in vivo* (Horswill et al., 2007). They display a contradictory pharmacological profile: increasing the specific binding of the CB_1 receptor agonist [^{3}H]CP55940 but produce a concentration-related decrease in CB_1 receptor agonist efficacy. The molecular mechanisms underlying this paradoxical pharmacological profile remain to be fully elucidated.

CB_1 receptors are coupled to the $G_{i/o}$ family of G proteins. Activation of these receptors leads to inhibition of adenylyl cyclases, and to phosphorylation and activation of mitogen-activated protein kinases (MAPK), including ERK1/2, (Turu and Hunyady, 2010). Following activation, β-arrestin molecules associate with phosphorylated CB_1 receptors. It is now accepted that a single receptor may engage different signalling pathways and that various ligands might influence these pathways differentially (Galandrin et al., 2007). This relatively new concept is termed 'functional selectivity' (Kenakin, 2007; Baker and Hill, 2010) and has been described for the CB_1 receptor (Anavi-Goffer, 2007; Glass and Northup, 1999; Mukhopadhyay and Howlett, 2001). This term can also be applied to allosteric modulators. If it is

Molecular Pharmacology Fast Forward. Published on November 15, 2012 as DOI: 10.1124/mol.112.080879
This article has not been copyedited and formatted. The final version may differ from this version.

supposed that numerous 'active' receptor conformations (leading to specific signalling outcomes) can be triggered by orthosteric agonists, then one might also postulate that any, but not always all, of these activation states may be stabilised by allosteric ligands. Allosteric ligands produce a distinctive receptor conformation which will possess a unique profile of pharmacology.

Recently, Ahn et al (2012) provided evidence that Org 27569 may behave as a CB_1 receptor biased ligand; acting as an allosteric agonist to induce receptor internalisation and ERK phosphorylation in a $G\alpha_i$-protein independent manner (PTX insensitive) whilst also acting as negative allosteric modulator of CB_1 agonist-mediated [^{35}S]GTPγS binding. Here we investigated the effects of allosteric modulators using a broad range of signalling endpoints linked to CB_1 receptor activation. We assessed the effects on CB_1 receptor agonist-induced (1) [^{35}S]GTPγS binding, which measures the level of G protein activation following agonist occupation of a GPCR (PTX sensitive), (2) inhibition of forskolin-stimulated cAMP production (Gαi-mediated, PTX sensitive) and stimulation of cAMP production (Gαs-mediated; revealed in presence of PTX) (3) phosphorylation of ERK1/2 (PTX sensitive) and (4) β arrestin recruitment (PTX insensitive). We find that Org 27569 *inhibits* agonist induced [^{35}S]GTPγS binding and β arrestin recruitment. It *inhibits* Gαi-mediated agonist-induced inhibition of cAMP production and Gαs-mediated stimulation of cAMP production. Alone the compound can act as an agonist, increasing cAMP production in untreated and PTX-treated cells. The compound acts as weak agonist alone inducing ERK phosphoryation in a PTX-sensitive manner; it *enhances* orthosteric agonist-induced ERK phosphorylation.

The level of cooperatively displayed by an allosteric compound is often ligand-dependent. There are well-documented differences in the ligand binding pocket for CB_1 receptor ligands which lead to ligand-specific conformational changes in the receptor (reviewed by Abood, 2005). An example is the W279$^{5.43A}$ mutation of the CB_1 receptor which reduces the binding of WIN55212 by 16-fold, but does not affect CP55940 binding (McAllister et al., 2003). Together with other residues, W5.43A has an important role in inducing ligand-selective CB_1 receptor activation (McAllister et al., 2003; McAllister et al., 2004). Here we find that Org 25769 and PSNCBAM-1

Molecular Pharmacology Fast Forward. Published on November 15, 2012 as DOI: 10.1124/mol.112.080879
This article has not been copyedited and formatted. The final version may differ from this version.

differentially modulate signalling of the CB_1 receptor agonists CP55940 and WIN55212, being significantly more potent as modulators of CP55940 signalling. Furthermore, in W5.43A mutated cells, Org 27569 loses the ability to inhibit CP55950 signalling.

In addition to signalling effects we have conducted an in depth characterisation of the effect of allosteric modulators on agonist binding; investigating the ability of these compounds to modulate radioligand binding in saturation, competition and kinetic binding assays. We found that in both saturation and kinetic binding experiments in brain membranes and hCB_1 expressing cells, both allosteric modulators appeared to influence only orthosteric ligand *maximum occupancy* rather than affinity.

Material and Methods

Materials

WIN55212, CP55940 and Org 27569 [5-Chloro-3-ethyl-1H-indole-2-carboxylic acid [2-(4-piperidin-1-yl-phenyl)-ethyl]-amide] were obtained from Tocris and SR141716A [N-(piperidin-1-yl)-5-(4-chlorophenyl)-1-(2,4-dichlorophenyl)-4-methyl-1H-pyrazole-3-carboxamide hydrochloride] from the National Institute on Drug Abuse. PSNCBAM-1 was synthesized by Prosidion Limited as described by Bloxham et al., (2006) (patent). Bovine serum albumin (BSA), Cell culture media, DTT, non-enzymatic cell dissociation solution, GDP, Gpp(NH)p, GTPγS, G418, l-glutamine, Krebs salts, penicillin/streptomycin, Tris Buffer and Triton X-100 were all obtained from Sigma-Aldrich. [^{3}H]CP55940 (128 Ci mmol^{-1}), [^{3}H]CP55940 (44 Ci mmol^{-1}) and [^{35}S]GTPγS (1250 Ci mmol^{-1}) were obtained from PerkinElmer Life Sciences Inc. (Boston, MA, USA). [^{3}H]SR141716A (43 Ci mmol^{-1}) was obtained from the National Institute on Drug Abuse.

CHO-hCB$_1$R cells

CHO cells stably transfected with cDNA encoding human cannabinoid CB_1 receptors (see Ross et al., 2009) were maintained in Dulbecco's modified Eagles's medium (DMEM) nutrient mixture F-12 HAM, supplemented with 2mM L-glutamine, 10% fetal bovine serum (FBS), 0.6% penicillin–streptomycin, hygromycin B (300μgml^{-1})

Molecular Pharmacology Fast Forward. Published on November 15, 2012 as DOI: 10.1124/mol.112.080879
This article has not been copyedited and formatted. The final version may differ from this version.

and geneticin (600μgml^{-1}). All cells were maintained at 37°C and 5% CO_2 in their respective media and were passage twice a week using non-enzymatic cell dissociation solution. The CHO-hCB_1R transfected cell line was used for cAMP, pERK1/2 and [^{35}S]GTPγS binding experiments.

HEK293-hCB1R cells

Untransfected HEK293 FlpIn™ tREx™ (Invitrogen Ltd.) cells were cultured in the following growth medium: Dulbecco's modified Eagle's medium (DMEM) containing 4.5g/L glucose, an L-glutamine substitute (Glutamax-1™), and supplemented with 10% fetal bovine serum, 50U/mL penicillin, 50μg/mL streptomycin, 15μg/mL blasticidin and 10μg/mL zeocin. Cells were grown in tissue culture flasks in an incubator at 37°C under 5% CO_2. A stable cell line that over-expresses the human CB_1 receptor when induced with tetracycline was created using the Flp-In™ tREx™ system (Invitrogen Ltd.) according to the manufacturer's instructions. HEK293 Flp-In™ tREx™ cells were transfected with the plasmid pcDNA5/FRT/TO (which contains a hygromycin resistance gene) into which the hCB1 receptor open reading frame had been inserted. A population of stable transfectants were selected by culturing cells in growth medium containing 100μg/mL hygromycin and 15μg/mL blasticidin. The HEK-hCB_1R cell line was used for radioligand binding studies.

Membrane Preparation

Mouse brain membrane preparation

Whole brains from adult male MF1 mice were suspended in centrifugation buffer (320 mM sucrose, 2 mM EDTA, 5 mM $MgCl_2$) and the tissues were homogenized with an Ultra-Turrex homogenizer. Tissue homogenates were centrifuged at 1600 g for 10 minutes and the resulting supernatant collected. This pellet was resuspended in centrifugation buffer centrifuged as before and the supernatant collected. Supernatants were combined before undergoing further centrifugation at 28,000 g for 20 minutes. The supernatant was discarded and the pellet resuspended in buffer A (50 mM Tris, 2 mM EDTA, 5 mM $MgCl_2$ at pH 7.0) and incubated at 37°C for 10 minutes. Following

Molecular Pharmacology Fast Forward. Published on November 15, 2012 as DOI: 10.1124/mol.112.080879
This article has not been copyedited and formatted. The final version may differ from this version.

the incubation, the suspension was centrifuged for 20 minutes at 23,000 g. After resuspending the pellet in buffer A, the suspension was incubated for 40 minutes at room temperature before a final centrifugation for 15 minutes at 11,000 g. The final pellet was resuspended in buffer B (50 mM Tris, 1 mM EDTA, 3 mM $MgCl_2$) and the final protein concentration, determined by Bio-Rad Dc kit, was 1 mg ml^{-1}. All centrifugation procedures were carried out at 4°C. Prepared brain membranes were stored at -80°C and defrosted on the day of the experiment.

Cell membrane preparation

A large batch of hCB_1R cells was prepared by expanding the cell culture to 20 220cm^2 flasks. To prepare cell membranes, cells were washed in PBS and then incubated with PBS containing 1mM EDTA for 5 min. Cells were then harvested by scraping into the buffer and centrifuged at 400 x g for 5 min. Cell pellets were then resuspended in ice-cold buffer A (320 mM sucrose, 10 mM HEPES, 1 mM EDTA, pH 7.4) and homogenized using a glass dounce homogenizer. Cell homogenates were then centrifuged at 1600 × g for 10 min at 4°C and the supernatant was collected. The pellet was re-suspended, homogenised and centrifuged at 1600 × g, and the supernatant was collected. Supernatants were pooled before undergoing further centrifugation at 50,000 × g for 2 h at 4°C. The supernatant was discarded and the pellet was re-suspended in buffer B (50 mM HEPES, 0.5 mM EDTA, 10 mM $MgCl_2$, pH 7.4), aliquoted into 0.5 mL tubes, and stored at -80°C. Protein concentration was determined against a BSA standard curve using BioRad Bradford protein detection reagent.

Signalling Assays

$[^{35}S]GTP\gamma S$ Binding Assay

Mouse brain membranes (5µg protein) or hCB_1R cell membranes (25µg protein) were preincubated for 30 minutes at 30°C with adenosine deaminase (0.5 U ml^{-1}). The membranes were then incubated with the agonist ± modulator or vehicle for 60

Molecular Pharmacology Fast Forward. Published on November 15, 2012 as DOI: 10.1124/mol.112.080879
This article has not been copyedited and formatted. The final version may differ from this version.

minutes at 30 °C in assay buffer (50 mM Tris-HCl; 50 mM Tris-Base; 5 mM $MgCl_2$; 1 mM EDTA; 100 mM NaCl; 1 mM DTT; 0.1% BSA) in the presence of 0.1 nM [^{35}S]GTPγS and 30 µM GDP, in a final volume of 500 µl. Binding was initiated by the addition of [^{35}S]GTPγS. Nonspecific binding was measured in the presence of 30 µM GTPγS. The reaction was terminated by rapid vacuum filtration (50 mM Tris-HCl; 50 mM Tris-Base; 0.1% BSA) using a 24-well sampling manifold (cell harvester; Brandel, Gaitherburg, MD) and GF/B filters (Whatman, Maidstone, UK) that had been soaked in buffer (50 mM Tris-HCl; 50 mM Tris-Base; 0.1% BSA) for at least 24 hours. Each reaction tube was washed five times with a 1.2 ml aliquot of ice-cold wash buffer. The filters were oven-dried for at least 60 minutes and then placed in 4 ml of scintillation fluid (Ultima Gold XR, Packard). Radioactivity was quantified by liquid scintillation spectrometry.

Data Analysis: Raw data were presented as cpm. Basal level was defined as zero. Results were calculated as a percentage change from basal level of [^{35}S]GTPγS binding (in the presence of vehicle). Data were analysed by nonlinear regression analysis of sigmoidal dose response curves using GraphPad Prism 5.0 (GraphPad, San Diego, CA). The results of this analysis are presented as E_{max} with 95% confidence limits and pEC_{50} ($logEC_{50}$) ± SEM.

PathHunter® CB_1 beta-arrestin assays

PathHunter® hCB_1 beta-arrestin cells were plated 48 hours before use and incubated at 37°C, 5% CO_2 in a humidified incubator. Compounds were dissolved in DMSO and diluted in OCC media. 5 µl of allosteric modulator or vehicle solution was added to each well and incubated for 60 minutes. 5 µl of agonist was added to each well followed by a 90 min incubation. 55 µl of detection reagent is then added followed by a further 90 min incubation at room temperature. Chemiluminescence, indicated as RLU, was measured on a standard luminescence plate reader.

Data Analysis: Raw data were relative light units (RLU). Basal level was defined as zero. Results were calculated as the percentage of CP55940 maximum effect. Data were analysed by nonlinear regression analysis of sigmoidal dose response curves using GraphPad Prism 5.0 (GraphPad, San Diego, CA). The results of this analysis are presented as E_{max} with 95% confidence limits and pEC_{50} ($logEC_{50}$) ± SEM.

Molecular Pharmacology Fast Forward. Published on November 15, 2012 as DOI: 10.1124/mol.112.080879
This article has not been copyedited and formatted. The final version may differ from this version.

Cyclic AMP assays

hCB_1R cells (0.6×10^5 $cells ml^{-1}$) were preincubated in phosphate buffered saline containing 1 mg ml BSA (assay buffer) for 30 min at 37°C with rolipram (10 μM). This was followed by further 30 minute incubation at 37°C with cannabinoid agonist ± Org 27569 or vehicle. A final incubation of 30 min with 5 μM forskolin in a total volume of 500 μl then took place. The reaction was terminated by addition 0.1 M HCl and centrifuged to remove cell debris. The pH was brought to 8 or 9 using 1 M NaOH and cyclic AMP content was then measured using a radioimmunoassay kit (The Biotrak™; Amersham). Forskolin and rolipram were dissolved in DMSO.

Data Analysis: Results were calculated as the percentage inhibition of forskolin-stimulated cAMP production (pmol mg^{-1}). Data were analysed by nonlinear regression analysis of sigmoidal dose response curves using GraphPad Prism 5.0 (GraphPad, San Diego, CA). The results of this analysis were presented as E_{max} with 95% confidence limits and pEC_{50} ($logEC_{50}$) ± SEM.

AlphaScreen® SureFire® ERK 1/2 phosphorylation assay

ERK1/2 MAP-kinase phosphorylation assay. For experimental studies of ERK1/2 MAP-kinase phosphorylation, hCB_1R cells (40,000 cells/well) were plated onto 96 well plates and serum-starved for 24 h. Cells were then washed with DMEM before the addition of agonist ± Org 27569 or vehicle at the desired concentration. After a 6 minute incubation at 37ºC in a humidified atmosphere, ice cold lysis buffer (provided with the AlphaScreen® SureFire® kit) was added to each well and the plate was placed at -80°C for at least 1 hour.

AlphaScreen® SureFire® ERK Assay. The assay was performed in 384 well white Proxiplates according to the manufacturer instructions. Briefly, 4 μl samples were incubated with 7 μl of mixture containing: 1 part donor beads: 1 part acceptor beads: 10 parts activation buffer: 60 parts reaction buffer. Plates were incubated for 3 hours at 25°C in the dark and read with the Envision® system (PerkinElmer) using AlphaScreen® settings.

Data Analysis. Raw data were presented as 'Envision units'. Basal level was defined as zero. Results were presented as means and variability as SEM or 95% confidence limits (CL) of the percent stimulation of phosphorylated ERK1/2 above the basal level (in the presence of vehicle). Data were analysed by nonlinear analysis of log

Molecular Pharmacology Fast Forward. Published on November 15, 2012 as DOI: 10.1124/mol.112.080879
This article has not been copyedited and formatted. The final version may differ from this version.

agonist versus-response curves using GraphPad Prism 5.0 (GraphPad, San Diego, CA). The results of this analysis were presented as E_{max} with 95% confidence limits and pEC_{50} ($logEC_{50}$) ± SEM.

Radioligand binding experiments

Competition and saturation binding assays

Mouse brain membranes

Binding assays were performed with the CB_1 receptor agonist, [^{3}H]CP55940 (0.7 nM for equilibrium or 0.1 to 10 nM for saturation) and CB_1 receptor agonist [^{3}H]WIN55212-2 (1.5 nM) in 1 mg ml^{-1} bovine serum albumin (BSA) and 50 mM Tris buffer, total assay volume 500 µl. Binding was initiated by the addition of mouse brain membranes (30 µg). Assays were carried out at 37 °C for 60 minutes before termination by addition of ice-cold wash buffer (50 mM Tris buffer, 1 mg ml^{-1} BSA) and vacuum filtration using a 24-well sampling manifold (Brandel Cell Harvester) and Whatman GF/B glass-fibre filters that had been soaked in wash buffer at 4°C for 24 h. Each reaction tube was washed five times with a 1.2 ml aliquot of buffer. The filters were oven-dried for 60 min and then placed in 4 ml of scintillation fluid (Ultima Gold XR, Packard), and radioactivity quantitated by liquid scintillation spectrometry. Specific binding was defined as the difference between the binding that occurred in the presence and absence of 1 µM of the corresponding unlabelled ligand and was 70 - 80% of the total binding.

hCB_1R cells

Saturation and competition binding assays were performed by incubating 5-10µg/well hCB_1R cell membranes in assay buffer (50 mM Tris, 2.5 mM EDTA, 5 mM $MgCl_2$, 1 mg mL^{-1} BSA, pH7.4) at 30°C for 90 min. Equilibrium binding assays were performed with [^{3}H]CP55940 (0.8 nM) or [^{3}H]WIN55212 (1.5 nM). Reactions were performed in duplicate or triplicate wells of 96-well, round bottom microtiter plates in a final volume of 200 µL. Following incubation, reactions were filtered onto GF/B filter mats pre-soaked in distilled H_2O using a PerkinElmer Filtermate™ cell harvester. Filters were washed 6 times with ice cold 50 mM Tris buffer (pH 7.4) then air-dried and the radioactivity counted in a Microbeta Trilux™ liquid scintillation counter.

Molecular Pharmacology Fast Forward. Published on November 15, 2012 as DOI: 10.1124/mol.112.080879
This article has not been copyedited and formatted. The final version may differ from this version.

Specific binding was defined as the difference between the binding that occurred in the presence and absence of 10 µM of unlabelled ligand.

Data Analysis: Saturation studies are generally carried out by measuring binding of a range of radioligand concentrations at equilibrium to a constant amount of receptor in the presence and absence of a high concentration of competing, unlabelled ligand. Specific binding data can then be analysed using the following model based on the Hill-Langmuir equation:

$$Y = \frac{B_{max} \times [A]}{[A] + K_d}$$

Here, Y is specific binding, B_{max} is the number of binding sites for the radioligand (A), K_d is the equilibrium dissociation constant for A, and [A] is the concentration of this radioligand at half the maximum occupancy.

Saturation binding assays thus provides the affinity of the radioligand for the receptor, which is the concentration of radioligand that produces half of the maximum binding (K_d), and the receptor density in the tissue under investigation which is the maximum level of specific binding (B_{max}). GraphPad Prism 5.0 (GraphPad, San Diego, CA) was used to calculate the K_d ± SEM and B_{max} values with 96% confidence limits.

Association and dissociation binding assays

Association binding experiments were performed by incubating 5-10 µg/well hCB_1R cell membranes with a fixed concentration (K_d or higher) of radioligand ([^{3}H]CP55940) in assay buffer (50 mM Tris, 2.5mM EDTA, 5 mM $MgCl_2$, 1mg mL^{-1} BSA, pH 7.4) at 30°C for various incubation times (1 min to 2 h) before termination of reactions by rapid filtration. For dissociation kinetic experiments, the radioligand was first incubated with membranes for 60 min to allow full association before an unlabelled competing ligand was added to each reaction at various time-points to initiate dissociation of the radioligand until reactions were terminated by filtration. Dissociation was initiated by the addition of 1µM unlabelled ligand in the presence and absence of test compounds. For both association and dissociation assays,

Molecular Pharmacology Fast Forward. Published on November 15, 2012 as DOI: 10.1124/mol.112.080879
This article has not been copyedited and formatted. The final version may differ from this version.

reactions were performed in duplicate or triplicate wells of 96-well, round bottom microtiter plates in a final volume of 200 µl. Following incubation, reactions were filtered onto GF/B filter mats pre-soaked in distilled H_2O using a PerkinElmer Filtermate™ cell harvester. Filters were washed 6 times with ice cold 50 mM Tris buffer (pH 7.4) then air-dried and the radioactivity counted in a Microbeta Trilux™ liquid scintillation counter.

Data Analysis: Kinetic binding assays can be used to calculate the association or dissociation rate constants of a radioligand. Association experimental data can be of use to establish the time of a radioligand to reach equilibrium and therefore provide an optimal incubation time for saturation or competition binding assays. Association experiments also provide an observed association rate, k_{obs} (the association rate at a given concentration of radioligand) and maximum receptor occupancy at equilibrium (Y_{max}). Dissociation experiments provide a dissociation rate constant for the radioligand, k_{off} which can be used with k_{obs} to calculate the association rate constant k_{on} using Equation below.

$$k_{on} = \frac{k_{obs} - k_{off}}{[A]}$$

Data were analysed using the one-phase association model in GraphPad Prism 5.0 (GraphPad, San Diego, CA) to calculate the k_{ob}± SEM, Y_{max} ± SEM, k_{off} ± SEM.

Statistical Analysis

Values have been expressed as means and variability as SEM or as 95% confidence limits. Mean values have been compared using Student's unpaired t test, One-sample tests, or analysis of variance (ANOVA) followed by Dunnett's test or the Newman-Keuls test. *P* values <0.05 were considered to be significant.

Molecular Pharmacology Fast Forward. Published on November 15, 2012 as DOI: 10.1124/mol.112.080879
This article has not been copyedited and formatted. The final version may differ from this version.

Results

Effect of allosteric modulators on CB_1 receptor agonist signalling

[^{35}S]GTPγS binding assay in brain membranes

In mouse brain membranes, CP55940 stimulated [^{35}S]GTPγS binding with a pEC_{50} value of 8.20 ± 0.11 and E_{max} of 62% (95% confidence limits of 56 and 69). The potency of WIN55212 (pEC_{50} = 7.84 ± 0.08) was not significantly different from that of CP55940, but the efficacy was significantly higher; E_{max} of 98% (95% confidence limits 90 and 107). Both allosteric modulators, Org 27569 and PSNCBAM-1 (Figure 1), produced a concentration-related reduction in the E_{max} values for both CP55490 and WIN55212 (Figure 2, Table 1). However, the compounds were significantly less effective as inhibitors of WIN55212 as compared to CP55940. Neither Org27569 nor PSNCBAM-1 significantly decreased the E_{max} of WIN55212 until a concentration of 1μM; in comparison the compounds inhibited the action of CP55940 at in the nM range (Figure 2; Table 1). Neither Org 27569 nor PSNCBAM-1 significantly altered the pEC_{50} values of CP55940 or WIN55212 at any of the concentrations tested (Table 1). Org 27569 alone had no significant effect on [^{35}S]GTPγS binding in mouse brain membranes at concentrations of 1 nM to 10 μM (data not shown).

Org 27569 also significantly decreased the efficacy of the endogenous cannabinoid anandamide (AEA) in this assay (Figure 2E; Table 1). The endocannabinoid was more susceptible to inhibition by the allosteric modulator than WIN55212; with significant inhibition being observed in the presence of 100nM Org 27569.

[^{35}S]GTPγS binding assay in hCB_1R cell membranes

In hCB_1 expressing cells, CP55940 stimulated [^{35}S]GTPγS binding with a pEC_{50} value of 7.35 ± 0.19 and E_{max} of 65% (95% confidence limits of 57 and 72). Neither the potency (pEC_{50} = 6.70 ± 0.17) nor the efficacy (E_{max} = 70.4 %, 95% confidence limits 61 and 79) of WIN55212 was significantly different from that of CP55940

Molecular Pharmacology Fast Forward. Published on November 15, 2012 as DOI: 10.1124/mol.112.080879
This article has not been copyedited and formatted. The final version may differ from this version.

(Figure 3). Org 27569 produced a concentration-related reduction in the E_{max} values for both CP55490 and WIN55212. However, the compound was significantly less effective as an inhibitor of WIN55212 as compared to CP55940 (Figure 3A and 3B, Table 2). In hCB_1R cells, Org 27569 behaved as a weak inverse agonist producing a small but significant decrease in basal [^{35}S]GTPγS binding at concentrations of 1 and 10 μM (Figure 3E). This effect was not observed in wild type CHO cells.

PSNCBAM-1 displayed a similar profile to that observed with Org 27569 (Figure 3C and 3D). The stimulation of [^{35}S]GTPγS binding induced by CP55940 was abolished by 300nM PSNCBAM-1. This concentration did not significantly affect the stimulation induced by WIN55212, the effect of which was only inhibited by micromolar concentrations of PSNCBAM-1.

Cyclic AMP assays in hCB_1R cell membranes

Next we measured the effect of Org 27569 on CB_1 agonist-mediated inhibition of forskolin stimulated cAMP production in hCB_1R cells (Figure 4A and 4B). In the presence of vehicle, CP55940 inhibited forskolin-stimulated cAMP formation with an E_{max} of 86.6% (95 % confidence limits 77 and 98) and pEC_{50} value of 8.01 ± 0.19. WIN55212 was significantly less potent with a pEC_{50} value of 7.02 ± 0.20 (Student's unpaired t-test) but had similar efficacy with an E_{max} of 78.5% (95 % confidence limits 64 and 93). Org 27569 significantly reduced the E_{max} for CP55940 at a concentration of 10 nM, with signalling being abolished in the presence of 100 nM of Org 27569 (P<0.001, one sample t-test) (Figure 4B, Table 2). In the presence of Org 27569 and CP55940 the level of cAMP was significantly lower than basal (Figure 4A). In contrast, Org 27569 was less effective as an inhibitor of WIN55212-mediated inhibition of forskolin stimulated cAMP production (Figure 4B, Table 2).

It has been previously demonstrated that CB1 receptors couple to both Gs and Gi proteins and can stimulate or inhibit the formation of cAMP; thus in the presence of PTX, a simulation of cAMP is revealed (Glass and Felder, 1997; Bonhous et al, 1998). In line with this we find that, after overnight treatment of hCB1R cells with PTX (5 ng ml^{-1}), CP55940 no longer inhibits but rather stimulates the production of

Molecular Pharmacology Fast Forward. Published on November 15, 2012 as DOI: 10.1124/mol.112.080879
This article has not been copyedited and formatted. The final version may differ from this version.

cAMP; the E_{max} for stimulation being 174% (95 % confidence limits 106 and 242) and the pEC_{50} being (5.87 ± 0.35). On the other hand, Org 27569 alone in the absence of PTX pre-treatment stimulates cAMP production, an effect that is maintained following PTX treatment (Figure 4C). The Emax for Org 27569 was 106% (95 % confidence limits 61 and 152) in the absence and 141% (95 % confidence limits 110 and 173) in the presence of PTX; The pEC_{50} values for Org 27569 was 5.87 ± 0.28 in the absence and 6.44 ± 0.23 in the presence of PTX. Neither Org 27569 nor CP55940 had any effect on forskolin-stimulated cAMP production in untransfected CHO cells Figure 4C). Notably, the CB1 receptor orthosteric inverse agonist, SR141 also produced an increase in cAMP levels (Emax of 50%, 95% confidence limits 32 - 68); an effect that was abolished after PTX pre-treatment indicating the effect was due to constitutive activation of Gi (Figure 4D).

The stimulation of cAMP produced by CP55940 in PTX pre-treated cells was abolished by 100nM Org 27569, a concentration which alone did not stimulate cAMP production (Figure 4E).

In the absence of forskolin, CP55940 produced a very small stimulation of cAMP production reaching an E_{max} of 11% (95% confidence limits of 7 – 14). Org 27569 did not significantly affected levels of cAMP in the absence of forskolin (Figure 4F).

ERK 1/2 phosphorylation assay in hCB1R cell membranes

Using an AlphaScreen® surefire® ERK 1/2 phosphorylation assay kit, we measured the effect of Org 27569 on activation of ERK 1/2 phosphorylation by CB_1 agonists in hCB_1R cells (Figure 5A and 5B). CP55940 induced rapid, transient ERK phosphorylation which peaked at 6 mins and rapidly decayed by 15-20 min (data not shown), this is similar to data obtained by others (Daigle et al., 2008). Subsequent analysis was conducted at the 6 minute time point. In the presence of vehicle, CP55940 induced ERK1/2 phosphorylation above basal with an E_{max} of 50.0% (95 % confidence limits 44 and 56) and pEC_{50} value of 7.69 ± 0.14. WIN55212 was significantly less potent with a pEC_{50} value of 6.95 ± 0.42 but its efficacy did not differ from that of CP55940: E_{max} value of 40.2 (95% confidence limits 27 and 54).

Molecular Pharmacology Fast Forward. Published on November 15, 2012 as DOI: 10.1124/mol.112.080879
This article has not been copyedited and formatted. The final version may differ from this version.

In contrast to the inhibitory effects observed with Org 27569 in the other signalling assays, at 100nM and 1μM this compound significantly ***increased*** the E_{max} for CP55940-induced ERK 1/2 phosphorylation (Figure 5A, Table 2). In the presence of 1μM Org 27569, the basal level of the CP55940 log concentration-response curve was 15% (95% confidence limits of 6 - 24). Org 27569 had no significant effect on ERK 1/2 phosphorylation induced by WIN55212 (Figure 5B, Table 2).

CP55940 did not induce ERK1/2 phosphorylation following pre-treatment of the cells for 24 hours with PTX (5 ng ml^{-1}) (Figure 5C). Org 27569 induced a small but significant level of ERK1/2 phosphorylation with an E_{max} of 19% (95 % confidence limits 11 and 26) and pEC_{50} value of 8.55 ± 0.99; the effect was abolished following PTX pre-treatment (Figure 5C).

PathHunter® beta-arrestin assays

In the PathHunter® beta-arrestin CB_1 assay (Figure 6, Table 3), CP55940 stimulated β arrestin recruitment with a pEC_{50} value of 7.89 ± 0.06 and E_{max} of 99% (95% confidence limits of 95 and 104). The potency of WIN55212 (pEC_{50} = 6.93 ± 0.14) was significantly lower than that of CP55940 (Student's unpaired t test), but the efficacy was not significantly different; E_{max} of 83% (95% confidence limits 70 and 97). The allosteric modulators, Org 27569 and PSNCBAM-1 produced a concentration-related reduction in the E_{max} values of both CP55490 and WIN55212 (Figure 6, Table 3). Neither Org 27569 nor PSNCBAM-1 significantly altered the pEC_{50} values of CP55940 or WIN55212 at any of the concentrations tested (Table 3). Org 25769 also significantly decreased the efficacy of the endogenous cannabinoid anandamide (AEA) in this assay (Figure 6E; Table 3). Org 27569 alone had no significant effect on β arrestin recruitment (Figure 6F).

As observed in the [^{35}S]GTPγS binding assay, the compounds were significantly less potent as inhibitors of WIN55212 as compared to CP55940. The IC_{50} values for the inhibitors were calculated from concentration-response curves of the inhibitor concentration versus the % reduction in the agonist E_{max} value. The IC_{50} values for

Molecular Pharmacology Fast Forward. Published on November 15, 2012 as DOI: 10.1124/mol.112.080879
This article has not been copyedited and formatted. The final version may differ from this version.

Org 27569 against CP55940 and WIN55212 (Figure 7) were 2.03 ± 0.37 nM and 10.17 ± 0.96 nM, respectively (P<0.001, Student's unpaired t test). Similarly, the IC_{50} values for PSNCBAM-1 against CP55940 and WIN55212 (Figure 7) were 2.72 ± 0.33 nM and 8.74 ± 0.78 nM, respectively (P< 0.001, Student's unpaired t test).

Single point mutation (W5.43A) of the CB_1 receptor

In view of the significant divergence of the effects of Org 27569 on CP55940 as compared to WIN55212, we investigated its effects in cells expressing the point mutation, W5.43A. McAllister et al., (2003) have demonstrated that WIN55212 is affected by W5.43A mutations, suggesting that these residues are part of the binding site for this ligand. In contrast, CP55940 is unaffected by this mutation. In wild type cells, 1 μM Org 27569 abolished CP55950 stimulation of [^{35}S]GTPγS binding. However, in the cells expressing the W5.43A point mutation of CB_1, Org 27569 (1 μM) did not significantly alter the E_{max} for CP55940-induced stimulation of [^{35}S]GTPγS binding (Supplementary Figure 2). These data suggest that there may be an overlap in the binding pocket for WIN55212 and Org 27569.

Effect of allosteric modulators on CB_1 receptor agonist binding

Equilibrium binding assays

In line with our previous studies (Price et al., 2005), we find that Org 27569 causes a significant and concentration-dependent increase in the specific binding of [^{3}H]CP55940 to mouse brain membranes with an E_{max} of 212 ± 11% and a pEC_{50} of 6.38 ± 0.21 (Figure 8A). Here we find that in mouse brain membranes PSNCBAM-1 similarly caused a 141 ± 7.9% increase in the specific binding of [^{3}H]CP55940 with a pEC_{50} of 6.87 ± 0.46 (Figure 8A). We have also previously reported (Price et al., 2005) that, in contrast to the increase in specific binding of [^{3}H]CP55940, Org 27569 caused a significant and concentration-related decrease in the specific binding of [^{3}H]SR141716A to mouse brain membranes; the displacement was incomplete and not consistent with a simple model of competitive displacement. We have also previously reported that, in hCB_1R cells, PSNCBAM-1 caused a significant and concentration-dependent, increase in [^{3}H]CP55940 binding of 159 ± 9% with a pEC_{50}

Molecular Pharmacology Fast Forward. Published on November 15, 2012 as DOI: 10.1124/mol.112.080879
This article has not been copyedited and formatted. The final version may differ from this version.

of 8.08 ± 0.20 (Horswill et al., 2007). In hCB_1R cells PSNCBAM-1 caused a significant and concentration-related decrease in the specific binding of [^{3}H]SR141716A with a pEC_{50} of 5.65 ± 0.07; the displacement was incomplete and not consistent with a simple model of competitive displacement (Horswill et al., 2007).

Here we have investigated the effect of both compounds on the specific binding of [^{3}H]WIN55212 for the first time. In mouse brain membranes preparations, Org 27569 had no significant effect on the specific binding of [^{3}H]WIN55212 at concentrations of up to 10 μM (Figure 8B). Unlabelled WIN55212 displaced [^{3}H]WIN55212 binding by 98 ± 4% with a pEC_{50} of 8.21 ± 0.11 (Figure 8B). PSNCBAM-1, at concentrations ranging from 1 nM to 10 μM, had a small but significant effect on the specific binding of [^{3}H]WIN55212 in mouse brain membranes (Figure 8B). In the presence of PSNCBAM-1 [^{3}H]WIN55212 binding was increased with an E_{max} of 124 % (95% confidence limits, 110 – 137) which is significantly different from 100%.

In hCB_1R cells PSNCBAM-1, at concentrations ranging from 1 nM to 10 μM, had a small but significant effect on the specific binding of [^{3}H]WIN55212. In the presence of PSNCBAM-1 [^{3}H]WIN55212 binding was increased to 109 % (95% confidence limits, 107 – 111) which is significantly different from 100% (Figure 8C). SR141716A fully inhibited [^{3}H]WIN55212 binding with a pK_i of 8.02 ± 0.08 (Figures 7C). This pK_i value was consistent with that reported for SR141against [^{3}H]CP55940 (pK_i of 8.35 ± 0.11) (Horswill et al., 2007).

These data demonstrate that PSNCBAM-1 and Org 27569 display ligand dependence exhibited in the level of binding cooperatively exhibited with [^{3}H]CP55940 and [^{3}H]WIN55212.

Molecular Pharmacology Fast Forward. Published on November 15, 2012 as DOI: 10.1124/mol.112.080879
This article has not been copyedited and formatted. The final version may differ from this version.

Saturation binding assays

Saturation binding experiments involved investigating the equilibrium dissociation constant (K_d) and maximum occupancy (B_{max}) of the CB_1 receptor agonist radioligand [^{3}H]CP55940. [^{3}H]CP55940 bound in a saturable manner to mouse brain membranes. (Figure 9A, Table 4). Org 27569 (1 μM and 10 μM) significantly increased the B_{max} of [^{3}H]CP55940 (Figure 8A, Table 4). However, the pK_d of [^{3}H]CP55940 was unaffected by Org 27569 at either concentration. Similarly, PSNCBAM-1 significantly increased the B_{max} value of [^{3}H]CP55940; neither 1 μM nor 10 μM PSNCBAM-1 significantly affected the pK_d of [^{3}H]CP55940 in mouse brain membranes, however there was a trend towards an increase in K_d (Figure 8B, Table 4). Similarly, in saturation experiments using hCB_1R membranes (Figure 8C, Table 4) the presence of 1 μM PSNCBAM-1 positively modulated binding of [^{3}H]CP55940 by increasing B_{max} (Table 4). However, the pK_d of [^{3}H]CP55940 was unaffected by PSNCBAM-1 (P>0.05, Student's *t* test).

This increase in B_{max} can be interpreted as an increase in the number of available binding sites for [^{3}H]CP55940. In parallel experiments, PSNCBAM-1 at 1 μM caused no change to the level of non-specific binding of [^{3}H]CP55940 (data not shown). Thus the effect on B_{max} would appear not to be a result of an increase in the level of non-specific binding.

Association and dissociation kinetics

Competition and saturation experiments at equilibrium showed Org 27569 and PSNCBAM-1 to *increase* the binding of radiolabelled agonists. To gain greater understanding of the mechanisms underlying this effect, further detailed analysis of the effects of one of these modulators (PSNCBAM-1) on agonist association and dissociation were carried out with [^{3}H]CP55940 in hCB_1R cells.

Molecular Pharmacology Fast Forward. Published on November 15, 2012 as DOI: 10.1124/mol.112.080879
This article has not been copyedited and formatted. The final version may differ from this version.

[^{3}H]CP55940 (0.5 nM) bound to hCB$_1$R membranes with an observed association rate constant (k_{ob}) of 0.060 ± 0.008 min^{-1} and a maximum receptor occupancy at equilibrium (Y_{max}) of 1.59 ± 0.10 pmol mg^{-1} (Figure 9C). When association of [^{3}H]CP55940 was measured in the presence of PSNCBAM-1 (2 μM), the compound had no effect on k_{ob}; values in being 6.0 ± 0.8 min^{-1} x 10^{-2} and 5.7 ± 0.4 min^{-1} x 10^{-2} in in DMSO and PSN treated respectively (P>0.05, Student's t test) but significantly elevated Y_{max} of [^{3}H]CP55940; values being 1.59 ± 0.1 pmolmg^{-1} and 2.46 ± 0.21 pmolmg^{-1} in DMSO and PSN treated respectively (P<0.05, Student's t-test); an increase of 55% which corresponds closely to previously observed effects for this compound in competition binding assays.

[^{3}H]CP55940 dissociated from CB$_1$ receptors in a bi-phasic manner in the absence of PSNCBAM-1 (data were best fitted to a two-phase dissociation curve) (Figure 9D). This was characterised by a fast phase during which 40.3 ± 1.9% of [^{3}H]CP55940 became dissociated, followed by a slow phase during which the remaining 59.7 ± 1.9% became dissociated. Approximately 20% of radioligand was not dissociated within the time of the experiment (120 min) but was predicted to become so from the trend of the curve. Such a bi-phasic relationship indicates that high and low affinity binding sites at the CB$_1$ receptor for [^{3}H]CP55940 are present in these membranes. A common explanation for this is that the fast phase corresponds to low affinity binding and thus the radioligand dissociates from the receptor quickly, whereas the slow phase corresponds to high affinity binding and thus the radioligand dissociates more gradually.

When PSNCBAM-1 was present during the dissociation phase at 0.1 μM and 2 μM it caused a significant concentration-dependent increase in the proportion of slow phase dissociation (Figure 9D and Table 5), such that its maximal effect produced 100% slow-phase dissociation (data were fitted best to a one-phase dissociation curve) (P<0.01, one-way ANOVA followed by Dunnett's multiple comparison). In the presence of 2 μM there was a slight alteration of the slow phase k_{off} for [^{3}H]CP55940. When present, the fast phase k_{off} was not significantly altered by 0.03 μM or 0.1 μM

Molecular Pharmacology Fast Forward. Published on November 15, 2012 as DOI: 10.1124/mol.112.080879
This article has not been copyedited and formatted. The final version may differ from this version.

PSNCBAM-1 (P>0.05, one-way ANOVA followed by Dunnett's multiple comparison) but was decreased marginally by 2 μM PSNCBAM-1 (P<0.05, one-way ANOVA followed by Dunnett's multiple comparison). Thus, PSNCBAM-1 appeared to increase the proportion of high affinity [^{3}H]CP55940 binding while not greatly affecting its dissociation rate.

Effects of Gpp(NH)p

Gpp(NH)p is a non-hydrolysable analogue of GTP and is known to cause uncoupling of G proteins from GPCRs. Such uncoupling of G proteins generally leads to a decrease in numbers of receptors in the high affinity agonist binding conformation, thus reducing agonist binding. To establish whether or not the ability of PSNCBAM-1 to increase [^{3}H]CP55940 binding was dependent on G proteins being associated with CB_1 receptors, binding experiments in the presence of Gpp(NH)p were performed. Gpp(NH)p caused a concentration-dependent decrease in [^{3}H]CP55940 binding to hCB_1R membranes. 100μM Gpp(NH)p decreased the pK_d of [^{3}H]CP55940 while apparently having little effect on B_{max} (Figure 10A); the pK_d values were 0.89 nM (95% confidence limits, 0.54 – 1.23) and 3.11 nM (95% confidence limits, 1.30 – 4.90) in the presence and absence of Gpp(NH)p respectively; the B_{max} values were 3.84 pmolmg^{-1} (95% confidence limits, 3.32 – 4.35) and 4.09 nM (95% confidence limits, 2.82 – 5.36) in the presence and absence of Gpp(NH)p respectively.

We also demonstrated that PSNCBAM-1 increases the B_{max} of [^{3}H]CP55940 in both brain membranes and hCB_1R cells (Figures 9A and B). The mechanism underlying this this increase in B_{max} remains to be established. However, one possible explanation for this increase is that it resulted from an increase in the number of receptors that are coupled to G protein - a condition that can give receptors higher affinity for agonist binding. If PSNCBAM-1 did indeed exert its effects through increased G protein association with receptors, then it might be expected to lose this property in the presence of Gpp(NH)p, in which receptors are uncoupled from G proteins. As displayed in Figure 10B, 100 μM Gpp(NH)p significantly reduced 0.5 nM [^{3}H]CP55940 binding by 46 ± 0.4% as would be predicted from the data displayed in Figure 10A (P<0.01, one-way ANOVA followed by Bonferroni's multiple comparison). Similar to results obtain in previous equilibrium binding experiments,

Molecular Pharmacology Fast Forward. Published on November 15, 2012 as DOI: 10.1124/mol.112.080879
This article has not been copyedited and formatted. The final version may differ from this version.

PSNCBAM-1 significantly increased [^{3}H]CP55940 binding by 59 ± 8% (P<0.01, one-way ANOVA followed by Bonferroni's multiple comparison). Surprisingly, when Gpp(NH)p was present, PSNCBAM-1 not only blocked the reduction in agonist binding caused by this agent, but also significantly increased the binding of [^{3}H]CP55940 by 35 ± 0.1% above its level of binding in the absence of Gpp(NH)p (P<0.01, one-way ANOVA followed by Bonferroni's multiple comparison). The difference between the effect of 1μM PSNCBAM-1 treatment in the presence and absence of Gpp(NH)p was not statistically significant indicating that Gpp(NH)p has little effect on agonist binding in the presence of PSNCBAM-1 (P>0.05, one-way ANOVA followed by Bonferroni's multiple comparison). Hence PSNCBAM-1 apparently retained its ability to increase [^{3}H]CP55940 binding even under conditions when CB_1 receptors would be expected to be uncoupled from G proteins.

As shown in Figure 10C, Gpp(NH)p (100 μM) affected [^{3}H]CP55940 dissociation by decreasing the slow phase of dissociation from 57.4 (95% confidence limits 54.6 and 59.8), to 29% (95% confidence limits 25 and 33). This effect was the opposite of that produced by PSNCBAM-1 which increased the slow phase of dissociation (Figure 9C). Like PSNCBAM-1, Gpp(NH)p caused only a small change in either the rapid or slow k_{off} values (Table 6). Hence Gpp(NH)p produced effects which are consistent with an decrease in the proportion of high affinity [^{3}H]CP55940 binding sites. As also shown in Figure 10C, in the presence of both PSNCBAM-1 (2 μM) and Gpp(NH)p (100 μM) the slow phase of [^{3}H]CP55940 dissociation was 58% (95% confidence limits 57 and 59) of total binding, a proportion which is very close to that in the absence of these agents. Again there was little change in the rapid or slow k_{off} values when both PSNCBAM-1 and Gpp(NH)p were present (Table 6). Thus, in dissociation experiments, PSNCBAM-1 appeared completely to reverse the effects of Gpp(NH)p (as was previously observed in equilibrium binding experiments).

Discussion

This study further highlights the unique pharmacological profile displayed by CB_1 receptor allosteric modulators. Here we present a comprehensive characterisation of

Molecular Pharmacology Fast Forward. Published on November 15, 2012 as DOI: 10.1124/mol.112.080879
This article has not been copyedited and formatted. The final version may differ from this version.

the effects of two allosteric modulators on a diverse range of CB_1 receptor coupled signalling pathways and on agonist binding kinetics. There are three major findings presented in this paper: these allosteric modulators display (1) ligand-dependent effects, (2) signalling pathway-dependent effects, and (3) effects on the maximum occupancy of CB_1 receptor agonists.

Studies have highlighted differences in the ligand recognition site for WIN55212 (and other aminoalkylindoles) and that of structurally-distinct agonists including CP55940 and anandamide (Abood, 2005; McAllister et al., 2003; Kapur et al., 2007). In particular, mutation of W5.43A results in a significant loss of affinity of WIN55212 and SR141716A, whilst the affinity of CP55940 was unaffected by this mutation (for review see Abood, 2005). In line with previous findings (Wang et al., 2011), here we show that the allosteric inhibitors display a marked ligand-selectively in a broad range of CB_1 receptor agonist signalling assays; both compounds are significantly less potent as inhibitors of WIN55212 signalling compared to CP55940 as measured in the [^{35}S]GTPγS, β arrestin and cAMP assays. We find that neither compound affects the specific binding of [^{3}H]WIN55212 at concentrations up to 10 μM. Furthermore, in cells expressing the CB_1 mutation, W5.43A, Org 27569 no longer inhibits CP55940-mediated signalling. Pharmacological and mutation studies also suggest a separation of the binding sites for the aminoalkylindoles from that of the other classes of cannabinoid ligands. For example the K3.28^{192} mutation has no effect on the affinity or efficacy of WIN55212 but causes a significant loss of affinity and efficacy of the other three classes of cannabinoid. In line with this, we find that the endocannabinoid, anandamide and CP55940 are equally susceptible to antagonism by Org 27569, whilst the effect on WIN55212 is divergent. Taken together, the data suggest some commonality in the binding pocket for WIN55212 and that of the allosteric modulators, the consequence being that WIN55212 is less susceptible to antagonism by these compounds. It is important to note that it is possible that this mutation may not affect the affinity of Org 27569, but might rather affect the ability of the CB1R to transmit cooperativity between CP55940 and Org27569. Further radioligand binding studies and studies directed at identifying the location and function of the allosteric binding pocket are in progress.

Molecular Pharmacology Fast Forward. Published on November 15, 2012 as DOI: 10.1124/mol.112.080879
This article has not been copyedited and formatted. The final version may differ from this version.

We also found that Org 27569 displays an intriguing profile of signalling pathway specificity. The compound produces a marked *inhibition* of CP55940-induced stimulation of [^{35}S]GTPγS binding in mouse brain membranes and hCB1R cells. Furthermore, it potently *inhibit* β arrestin recruitment, which is PTX insensitive. Org 27569 also apparently *inhibits* Gαi-mediated CP55940-induced inhibition of forskolin-stimulated cAMP production. As previously show by others (Glass and Felder, 1997; Bonhaus et al, 1998; Chen et al, 2010), pre-treatment of CB1R expressing cells with PTX, unmasks CB1 receptor-mediated, Gαs coupled stimulation of cAMP production; Org 27569 (100nM) also abolished CP55940-induced increases in cAMP production. However, Org 27569 alone (at concentrations above 100nM) stimulated cAMP production; an effect that was unaffected by PTX pre-treatment. Org 27569 had no effect on cAMP levels in the absence of forskolin. It is known that forkolin and Gαs synergise to activate adenylyl cylase (Glass & Felder, 1997; Barovsky & Brooker, 1985). Taken together, the data suggest that Org 27569 can act both as a CB1 receptor *allosteric agonist* of Gαs coupled CB1 receptor signalling and (at lower concentrations) as an *allosteric inhibitor* of orthosteric agonist induced activation of Gαs signalling. It is unlikely that the increase in cAMP observed with Org 27569 is inverse agonism of Gαi-mediated signalling because the effect is unaffected by PTX treatment. In contrast, the increase in cAMP observed with the CB1 receptor inverse agonist, SR141716A is abolished by PTX pre-treatment. Because the Org 27569 increases cAMP alone, it is not possible to conclude if the inhibition by this compound of CPP55940-induced inhibition of cAMP, is due to inhibition Gαi- signalling or simply 'physiological antagonism' due to concomitant activation of Gαs.

In contrast to the inhibition of orthosteric agonist signalling observed in other assays, Org 27569 *enhances* CP55940 induced ERK phosphorylation. As observed for Gαs mediated increases in cAMP, Org 27569 can also act as an allosteric agonist (low efficacy) to induce ERK phsophorylation; an effect which is Gαi mediated because this effect is lost in the presence of PTX.

Ahn et al., (2012) have recently reported that Org 27569 acts as an inhibitor of both basal and agonist-induced G protein coupling in a [^{35}S]GTPγS assay. However, Ahn

Molecular Pharmacology Fast Forward. Published on November 15, 2012 as DOI: 10.1124/mol.112.080879
This article has not been copyedited and formatted. The final version may differ from this version.

et al., (2012) found that this compound alone, at the high concentration of 10 μM, promotes receptor internalization and increases ERK phosphorylation. Furthermore, the effects on pERK seemed to be G-protein independent (PTX insensitive). We also find that Org 27569 alone acts as a weak inverse agonist in the [^{35}S]GTPγS assay but apparently as an agonist of Gαs signalling and a weak partial agonist of Gαi signalling in pERK assays respectively. Furthermore we find that this compound alone has no effect on β arrestin recruitment, which is known to be PTX insensitive (Lee et al., 2009), but does act as an inhibitor of CB_1 agonist-induced β arrestin recruitment. In line with finding of Ahn et al (2012), we also identify marked divergence of the effect of Org 27569 on CB_1 receptor agonist-induced ERK phosphorylation, whereby Org 27569 (100 nM and 1 μM) significantly *increases* the efficacy (E_{max}) of CP55940 as compared to inhibition observed in all other assays. Notably the ERK phosphorylation induced by CP55940 and Org 27569 is abolished after PTX treatment. Other have previously demonstrated that Cb1 mediated ERK phosphorylation is Gαi mediated (Chen et al, 2010); Our results present a fascinating pharmacological profile for Org 27569, which apparently traffics CB_1 mediated signalling, potentially inhibiting orthosteirc agonist mediated cellular events mediated by cAMP and β arrestin whilst enhancing CB_1 pERK-mediated cellular events.

There are well-documented examples of agonist-selective CB_1 receptor coupling (reviewed by Bosier et al., 2010). For example, in the mouse tetrad WIN55212 is more potent in reducing mobility and than in producing antinociception, whereas CP 55940 is significantly more potent in reducing motor activity than producing catalepsy. Agonist-selective signalling or pharmacodynamic variations may underlie these ligand differences. Reports have identified the CB_1 activated ERK signalling cascade as a key mediator of several forms of cocaine induced synaptic plasticity thereby implicating this cascade in addiction (Pan et al., 2011). It is conceivable that a CB_1 receptor allosteric modulator may be designed which selectively modulates pERK, thus providing a more targeted treatment for addiction. To our knowledge, the differential effects of Org 27569 described in this paper provide the first example of signal transduction-related *biased antagonism* of CB_1-receptor signalling.

Molecular Pharmacology Fast Forward. Published on November 15, 2012 as DOI: 10.1124/mol.112.080879
This article has not been copyedited and formatted. The final version may differ from this version.

In an effort to understand the nature of the receptor modulation induced by Org 27569 and PSNCBAM-1 we carried out saturation binding studies. In these experiments both allosteric modulators surprisingly caused an elevation in B_{max} of [^{3}H]CP55940, indicating an increase in the number of available binding sites in the presence of these compounds. We observed no significant change in agonist affinity (K_d). This contrasts with the Org 27569-induced increase in [^{3}H]CP55940 affinity with no change in maximum occupancy reported recently by Ahn et al (2012), although notably, they did observe a trend towards an increase in B_{max} in the presence of Org 27569.

In kinetic binding assays with [^{3}H]CP55940 in CB1R cells, it appears that 60% of the CB_1 receptors occupied by CP55940 are G protein-coupled (slow dissociation phase, high affinity), whereas the remaining 40% are uncoupled (fast dissociation phase, low affinity). The fact that the G protein uncoupling agent Gpp(NH)p reduced the slow phase of binding, and thus the fraction of receptors coupled to G proteins, supports this hypothesis. In hCB_1R membranes, PSNCBAM-1 did not significantly affect either the observed association rate constant (k_{ob}) or dissociation rate constant (k_{off}) of [^{3}H]CP55940, but instead exerted a substantial effect on the proportions of fast and slow phases of dissociation. The k_{off} of a ligand is highly reflective of its binding affinity and therefore any alteration of k_{off} by a modulator may indicate a change in ligand affinity. The lack of substantial PSNCBAM-1 effects on CP55940 k_{ob} and k_{off} implies that this compound causes very little alteration in CP55940 affinity. These results are consistent with saturation binding experiments at equilibrium where neither modulator altered the K_d of [^{3}H]CP55940. In contrast, the slow phase of CP55940 dissociation was greatly augmented from 60% in the absence of PSNCBAM-1 to 100% at the maximum PSNCBAM-1 concentration of 2 μM. Thus, consistent with the increase in B_{max} observed in saturation binding assays, the presence of PSNCBAM-1 in kinetic assays appears to cause an *increase in the proportion* of high affinity agonist binding sites.

Strikingly, PSNCBAM-1 retained its ability to augment CP55940 binding, even in the presence of Gpp(NH)p and blocked Gpp(NH)p effects on CP55940 dissociation. Hence, while Gpp(NH)p produced the expected effect of reducing agonist binding by

Molecular Pharmacology Fast Forward. Published on November 15, 2012 as DOI: 10.1124/mol.112.080879
This article has not been copyedited and formatted. The final version may differ from this version.

uncoupling G proteins, PSNCBAM-1 effectively opposed this action in both equilibrium and kinetic binding experiments. This property of PSNCBAM-1 is consistent with its ability to increase the maximal number of binding sites (B_{max}). Thus, even under conditions when G proteins would not be expected to be associated with CB_1 receptors, PSNCBAM-1 apparently induces a receptor conformation which displays a high affinity towards agonist compounds.

Previous investigations have demonstrated that structurally distinct ligands regulate CB_1 receptor-G-protein complexes with Gαi1, Gαi2, and Gαi3 such that multiple conformations of the receptor can be evoked by ligands to regulate individual G proteins (Mukhopadhyay and Howlett, 2005, Anavi-Goffer et al., 2009). Mukhopadhyay and Howlett, (2005) found that the non-hydrolysable GTP analogue, GTPγS, promoted complete dissociation of all CB_1 receptor-Gαi complexes; the CB1 agonist, desacetyllevonantradol, precluded GTPγS-induced dissociation of Gαi3, whilst leaving Gαi1 dissociation unaffected. In contrast, WIN55212 did not affect GTPγS-induced dissociation of any of the Gαi subtypes, which is consistent with the non-selectivity of this cannabinoid for Gαi subtypes. It is conceivable that the biased antagonism observed here reflects the fact that allosteric modulators facilitate interactions with specific Gα subtypes while impeding interactions with others. The increase in B_{max} may be indicative of a high affinity coupled complex that is coupled to a unique Gα pool which displays biased signalling. Differential effects of allosteric modulators on CP55940 and WIN55212 may also reflect differential Gα coupling of the agonist-allosteric bound receptor and warrant future investigation. Georgieva et al., (2008) found that CP55940 and WIN55212-bound CB_1 receptor conformations have similar affinities for Giα1 but are profoundly different in their ability to activate this G protein type, WIN55212 being significantly more active. The finding presented here indicted that the modulators may promote the binding of a G protein subtype that binds to the CP-bound, but not the WIN-bound receptor

Overall radioligand binding experiments indicate that the allosteric modulators, Org 27569 and PSNCBAM-1, may be able to make available a population of CB_1 receptors that retains the ability to bind agonists with high affinity, but that is not

Molecular Pharmacology Fast Forward. Published on November 15, 2012 as DOI: 10.1124/mol.112.080879
This article has not been copyedited and formatted. The final version may differ from this version.

active in terms of its capacity to trigger certain CB1 agonist signalling responses. This hypothesis, that Org 27569 induces a high affinity non-signalling state, is also supported by data obtained by Ahn et al (2012). Our data prompt an extension to this hypothesis, which is that in some functional assays the formation of the same complex will result in a loss of coupling to certain signalling pathways (cAMP, β arrestin) but simultaneously enhance signalling mediated by ERK phosphoryation. In addition, we find that Org 27569 alone can act as an *allosteric agonist*, activating both Gαi and Gαs mediated cellular responses. Taken together, the data suggest a model in which the binding of the modulators to the allosteric site stabilises a CB1 receptor conformation which is capable of inducing Gα-dependent signalling. It may be that this conformation mimics the GTP bound conformation and this precludes receptor uncoupling by Gpp(NH)p. As expected, this conformation has high affinity for the orthosteric agonist but inhibits orthosteric agonist signalling via certain Gα mediated pathways (see Figure 11).

Molecular Pharmacology Fast Forward. Published on November 15, 2012 as DOI: 10.1124/mol.112.080879
This article has not been copyedited and formatted. The final version may differ from this version.

Authorship Contribution

Participated in the research design: Baille, Horswill, Reggio, Abood, Anavi-Goffer, Strange, Stephens, Pertwee, Ross.

Conducted experiments: Baille, Horswill, Bolognini.

Contributed to new reagents or analytical tool: Reggio, Abood, McAllister.

Performed data analysis: Baillie, Horswill, Ross.

Wrote or contributed to writing manuscript: Baille, Horswill, Reggio, Abood, Anavi-Goffer, Stephens, Pertwee, Ross.

Molecular Pharmacology Fast Forward. Published on November 15, 2012 as DOI: 10.1124/mol.112.080879
This article has not been copyedited and formatted. The final version may differ from this version.

References

Abood ME, (2005) Molecular biology of cannabinoid receptors. *Handbook Experimental Pharmacology* **168**:81-115

Ahn KH, Mahmoud MM, Kendall DA, (2012)Allosteric modulator ORG27569 induces CB1 cannabinoid receptor high affinity agonist binding state, receptor internalization, and Gi protein-independent ERK1/2 kinase activation. *J Biol Chem* **287**:12070-82.

Anavi-Goffer S, Fleischer D, Hurst DP, Lynch DL, Barnett-Norris J, Shi S, Lewis DL, Mukhopadhyay S, Howlett AC, Reggio PH, Abood ME (2007) Helix 8 Leu in the CB1 cannabinoid receptor contributes to selective signal transduction mechanisms. *J Biol Chem*. **282**:25100-13.

Baker JG, Hill SJ. (2007) Multiple GPCR conformations and signalling pathways: implications for antagonist affinity estimates. *Trends Pharmacol Sci* **28**:374-81.

Bonhaus DW, Chang LK, Kwan J, Martin GR. (1998). Dual activation and inhibition of adenylyl cyclase by cannabinoid receptor agonists: evidence for agonist-specific trafficking of intracellular responses. *J Pharmacol Exp Ther*. **287**:884-8.

Barovsky K, Brooker G (1985) Forskolin potentiation of cholera toxin stimulated cyclic-AMP accumulation in intact C6–2B cells. Evidence for enhanced Gs-C coupling. *Mol Pharmacol* **28**:502–507.

Bosier B, Muccioli GG, Hermans E, Lambert DM (2010) Functionally selective cannabinoid receptor signalling: therapeutic implications and opportunities. *Biochem Pharmacol* **80**:1-12.

Chen XP, Yang W, Fan Y, Luo JS, Hong K, Wang Z, Yan JF, Chen X, Lu JX, Benovic JL, Zhou NM. (2010). Structural determinants in the second intracellular loop of the human cannabinoid CB1 receptor mediate selective coupling to G(s) and G(i). *Br J Pharmacol*. **161**:1817-34.

Daigle TL, Kearn CS, Mackie K (2008) Rapid CB1 cannabinoid receptor desensitization defines the time course of ERK1/2 MAP kinase signaling. *Neuropharmacol* **54**:36-44.

Galandrin, S., Oligny-Longpre, G. & Bouvier, M. (2007) The evasive nature of drug efficacy: implications for drug discovery. *Trends in Pharmacol Sci* 28: 423-430.

Georgieva T, Devanathan S, Stropova D, Park CK, Salamon Z, Tollin G, Hruby VJ, Roeske WR, Yamamura HI, Varga E (2008) Unique agonist-bound cannabinoid CB1 receptor conformations indicate agonist specificity in signaling. *Eur J Pharmacol* **581**:19-29.

Glass M, Felder CC. (1997). Concurrent stimulation of cannabinoid CB1 and dopamine D2 receptors augments cAMP accumulation in striatal neurons: evidence for a Gs linkage to the CB1 receptor. *J Neurosci.* **17**:5327-33.

Glass M, Northup JK, (1999) Agonist selective regulation of G proteins by cannabinoid CB(1) and CB(2) receptors. *Mol Pharmacol* **56**:1362-9.

Hall DA (2000) Modeling the functional effects of allosteric modulators at pharmacological receptors: an extension of the two-state model of receptor activation *Mol Pharmacol* **58**: 1412-1423.

Horswill, JG, Bali U, Shaaban S, Keily JF, Jeevaratnam P, Babbs AJ, Reynet C, Wong Kai In, P. (2007) PSNCBAM-1, a novel allosteric antagonist at cannabinoid CB1 receptors with hypophagic effects in rats. *Br J Pharmacol* **152**: 805-814.

Kapur A, Hurst DP, Fleischer D, Whitnell R, Thakur GA, Makriyannis A, Reggio PH, Abood ME (2007) Mutation studies of Ser7.39 and Ser2.60 in the human CB1 cannabinoid receptor: evidence for a serine-induced bend in CB1 transmembrane helix 7. Mol Pharmacol. 71:1512-24.

Kenakin T (2007) Collateral efficacy in drug discovery: taking advantage of the good (allosteric) nature of 7TM receptors. *Trends in Pharmacol Sci* **28**: 407-415.

McAllister SD, Rizvi G, Anavi-Goffer S, Hurst DP, Barnett-Norris J, Lynch DL, Reggio PH, Abood ME. (2003) An aromatic microdomain at the cannabinoid CB(1) receptor constitutes an agonist/inverse agonist binding region. *J Med Chem* **46**:5139–5152.

McAllister SD, Hurst DP, Barnett-Norris J, Lynch D, Reggio PH, Abood ME. (2004) Structural mimicry in class A G protein-coupled receptor rotamer toggle switches: the importance of the F3.36(201)/W6.48(357) interaction in cannabinoid CB1 receptor activation. J Biol Chem. 279:48024-37.

Mathiesen JM, Ulven T, Martini L, Gerlach LO, Heinemann A, Kostenis E (2005) Identification of indole derivatives exclusively interfering with a G protein-independent signaling pathway of the prostaglandin D2 receptor CRTH2. *Mol Pharmacol*, **68**: 393-402.

Mukhopadhyay S, Howlett AC (2001) CB1 receptor-G protein association. Subtype selectivity is determined by distinct intracellular domains. *Eur J Biochem* **268**:499-505.

Nathan PJ, O'Neill BV, Napolitano A, Bullmore ET (2011) Neuropsychiatric adverse effects of centrally acting antiobesity drugs. *CNS Neuro Therap* **17**:490-505.

Pan B, Zhong P, Sun D, Qing-song L, (2011) Extracellular Signal-Regulated Kinase Signaling in the Ventral Tegmental Area Mediates Cocaine-Induced Synaptic Plasticity and Rewarding Effects. *J Neurosci*. **31**: 11244-11255

Price MR, Baillie GL, Thomas A, Stevenson LA, Easson M, Goodwin R, McLean A, McIntosh L, Goodwin G, Walker G, Westwood P, Marrs J, Thomson F, Cowley P, Christopoulos A, Pertwee RG, Ross RA (2005) Allosteric modulation of the cannabinoid CB1 receptor. *Mol Pharmacol* **68**:1484-1495.

Ross RA, Brockie HC, Stevenson LA, Murphy VL, Templeton F, Makriyannis A, Pertwee RG (1999) Agonist-inverse agonist characterization at CB1 and CB2 cannabinoid receptors of L759633, L759656, and AM630. *Br J Phamraocl* **126**:665-72.

Ross, R.A. 2007, Allosterism and cannabinoid CB(1) receptors: the shape of things to come, *Trends Pharmacol Sci* **28**: 567-572.

Turu G, Hunyady L (2010) Signal transduction of the CB1 cannabinoid receptor. *J Mol Endocrinol* **44**:75-85.

Wang X, Horswill JG, Whalley BJ, Stephens GJ (2011) Effects of the allosteric antagonist 1-(4-chlorophenyl)-3-[3-(6-pyrrolidin-1-ylpyridin-2-yl)phenyl]urea (PSNCBAM-1) on CB1 receptor modulation in the cerebellum. *Mol Pharmacol* **79**:758-67

Molecular Pharmacology Fast Forward. Published on November 15, 2012 as DOI: 10.1124/mol.112.080879
This article has not been copyedited and formatted. The final version may differ from this version.

FOOTNOTES

These authors made an equal contribution to the work: Gemma L Baillie and James Horswill.

Financial support: The work was funded by Prosidion Inc and National Institutes of Health [Grants DA003934 and DA023204].

Molecular Pharmacology Fast Forward. Published on November 15, 2012 as DOI: 10.1124/mol.112.080879
This article has not been copyedited and formatted. The final version may differ from this version.

Legends

Figure 1: Structures of Org 27569 (Org) and PSNCBAM-1 (PSN).

Figure 2: [^{35}S]GTPγS binding to mouse brain membranes: (A) the effect of Org 27569 on CP55940; (B) the effect of Org 27569 on WIN55212; (C) the effect of PSNCBAM-1 on CP55940; (D) the effect of PSNCBAM-1 on WIN55212; (E) the effect of Org 27569 on Anandamide (AEA). Symbols represent mean values ± SEM from 3 to 4 experiments carried out in duplicate.

Figure 3: [^{35}S]GTPγS binding to hCB1 expressing cells: (A) the effect of Org 27569 on CP55940; (B) the effect of Org 27569 on WIN55212; (C) the effect of PSNCBAM-1 on CP55940; (D) the effect of PSNCBAM-1 on WIN55212; (E) the effect of Org 27569 alone in hCB1 cells and non-transfected cells. Symbols represent mean values ± SEM from 3 to 4 experiments carried out in duplicate.

Figure 4: Cyclic AMP production in hCB_1 expressing cells. (A) Effect of Org 27569 on CP55940-induced inhibition of forskolin-stimulated cAMP production (***P<0.001, **P<0.01, significance of difference from basal, one sample t-test); (B) Effect of Org 27569 on WIN55212-induced inhibition of forskolin-stimulated cAMP production (C) Effect of CP55940 and Org 27569 alone on forskolin-stimulated cAMP production in cells treated with vehicle or PTX (5 ng ml^{-1}, 24 hours) (D) Effect of SR141716A alone on forskolin-stimulated cAMP production in cells treated with vehicle or PTX (5 ng ml^{-1}, 24 hours) (E) Effect of Org 27569 (100nM) on the stimulation of cAMP production (in the presence of forskolin) produced by CP55940 in cells treated with PTX (5 ng ml^{-1}, 24 hours) (F) Effect of Org 27569 and CP55940 on cAMP production in the absence of forskolin. Symbols represent mean values ± SEM from 3 to 6 experiments carried out in duplicate.

Figure 5: ERK phosphorylation in hCB_1 expressing cells. (A) Effect of Org 27569 on CP55940 induced ERK phosphorylation (B) Effect of Org 27569 on WIN55212

Molecular Pharmacology Fast Forward. Published on November 15, 2012 as DOI: 10.1124/mol.112.080879
This article has not been copyedited and formatted. The final version may differ from this version.

induced ERK phosphorylation (C) Effect of CP55940 and Org 27569 alone on ERK phosphorylation in cells treated with vehicle or PTX (5 ng ml^{-1}, 24 hours).

Figure 6: PathHunter® β arrestin assay performed with hCB_1 cells: (A) the effect of Org 27569 on CP55940; (B) the effect of Org 27569 on WIN55212; (C) the effect of PSNCBAM-1 on CP55940; (D) the effect of PSNCBAM-1 on WIN55212; (E) the effect of Org 27569 on Anandamide (AEA); (F) The effect of Org 27569 alone. Symbols represent mean values ± SEM from 2 to 4 experiments carried out in duplicate.

Figure 7: Comparison of IC_{50} values for Org 27569 and PSNCBAM-1 as inhibitors of CP55940, WIN55212 and Anandamide in the β arrestin assay performed with hCB_1 cells. Columns represent mean values ± SEM from 3 to 4 experiments carried out in duplicate. The IC_{50} values (nM) were obtained using Prism 5 to construct concentration-response curves of the inhibitor concentration versus the % reduction in each agonist E_{max} value.

Figure 8: Effect of allosteric modulators on the equilibrium binding: (A) effect of Org 27569 and PSNCBAM-1 on [^{3}H]CP55940 binding to mouse brain membranes (B) effect of Org 27569 and PSNCBAM-1 on [^{3}H]WIN55212 binding to mouse brain membranes and (B) effect of PSNCBAM-1 on [^{3}H]WIN55212 binding to hCB_1R cell membranes. Symbols represent mean values ± SEM from 3 independent experiments. Data were best fitted by a one-site competition binding model. * $P<0.05$, ** $P<0.01$, one-sample *t*-test.

Figure 9: Effect of (A) Org 27569 on saturation binding of [^{3}H]CP55940 in mouse brain membranes (B) PSNCBAM-1 on saturation binding of [^{3}H]CP55940 in mouse brain membranes. Data shown are mean ± SEM 5 independent experiments. Data were best fitted by a one-binding site saturation model. (C) PSNCBAM-1 on saturation binding of [^{3}H]CP55940 in hCB_1 cell membranes. Data shown are mean ± SEM of triplicate wells from a representative experiment that was performed 3 times. Data were best fitted by a one-binding site saturation model. The B_{max} and K_d from 3 independent experiments are shown in Table 4. (D) PSNCBAM-1 on [^{3}H]CP55940

Molecular Pharmacology Fast Forward. Published on November 15, 2012 as DOI: 10.1124/mol.112.080879
This article has not been copyedited and formatted. The final version may differ from this version.

(0.5 nM) association kinetics in hCB_1 cell membranes. Data were best fitted by a one-phase association model. Data shown are mean values ± SEM of triplicate wells from a single representative experiment that was performed 3 times. The k_{ob} and Y_{max} parameters from three independent experiments are presented in Table 5. (E) PSNCBAM-1 on [^{3}H]CP55940 (0.5nM) dissociation kinetics in hCB_1 cell membranes. Data shown are mean values ± SEM from 3 independent experiments. Data were best fitted by a two-phase dissociation model. Data for 2 μM PSNCBAM-1 were best fitted by a one-phase dissociation model. Phase proportions and k_{off} values for three independent experiments are displayed in Table 6.

Figure 10: Effect of Gpp(NH)p and/or PSNCBAM-1 (1μM) in hCB_1R cell membranes on (A) saturation binding of [^{3}H]CP55940; (B) [^{3}H]CP55940 equilibrium binding; (C) [^{3}H]CP55940 dissociation. Data shown in A are mean values ± SEM of triplicate wells from a single experiment that was performed twice. Data were best fitted using a one-site saturation binding model. Data shown in B are mean values ± SEM from 3 independent experiments. $^{**}P<0.01$, $\#P>0.05$; one-way ANOVA followed by Bonferroni's multiple comparison. Data shown in C are mean values ± SEM of triplicate wells, the experiment was performed twice. Data for all groups were best fitted using a two-phase dissociation model. Phase proportions and k_{off} values are displayed in Table 7.

Figure 11: Figure summarizing the complex pharmacology of the CB1 receptor allosteric modulators. The left panel shows the effect of Org 27569 alone and on the right, the effect of Org 27569 on binding and signaling of the CB1 receptor orthosteric ligand, CP55940.

Molecular Pharmacology Fast Forward. Published on November 15, 2012 as DOI: 10.1124/mol.112.080879
This article has not been copyedited and formatted. The final version may differ from this version.

Table 1: Effect of Org 27569 and PSNCBAM-1 on CP55940 and WIN55212-2 stimulated [^{35}S] GTPγS binding in mouse brain membranes. Data are mean ± SEM or with 95% confidence limits (CL)

Agonist	Vehicle/modulator	pEC_{50} [a]	E_{max} [b] (%) (95% CL)	% Inhibition ± S.E.M
CP55940	**DMSO**	8.2 ± 0.1	62.6 (57 - 69)	
	Org 27569 (10 nM)	7.9 ± 0.3	43.5 (31 - 56) †	33.9 ± 6.7
	Org 27569 (100 nM)	8.6 ± 0.4	17.98 (12 - 24) †	71.8 ± 7.0
	Org 27569 (1 µM)	-	-	95.3 ± 6.6
WIN55212	**DMSO**	7.8 ± 0.09	98.9 (90 - 107)	
	Org 27569 (10 nM)	7.7 ± 0.2	83.1 (68 - 98)	13.9 ± 8.4
	Org 27569 (100 nM)	8.0 ± 0.2	90.0 (75 - 105)	8.7 ± 13.3
	Org 27569 (1 µM)	8.4 ± 0.3	35.9 (27 - 45) †	63.6 ± 4.2
Anandamide	**DMSO**	6.7 ± 0.1	61.4 (55 – 68)	
	Org 27569 (10 nM)	6.7 ± 0.4	56.6 (33 – 80)	1.1 ± 12.5
	Org 27569 (100 nM)	6.4 ± 0.2	39.0 (30 – 48) †	38.1 ± 3.8
	Org 27569 (1 µM)	7.6 ± 0.3	17.2 (13 – 22) †	71.9 ± 3.4
CP55940	**DMSO**	7.0 ± 0.2	53.7 (47 - 60)	
	PSN (10 nM)	6.5 ± 0.2	48.7 (39 - 58)	7.1 ± 12.7
	PSN (100 nM)	6.6 ± 0.4	32.6 (24 - 41) †	41.8 ± 9.6
	PSN (1 µM)	6.0 ± 0.5	15.6 (6 - 25) †	72.8 ± 8.4
WIN55212	**DMSO**	7.8 ± 0.1	75.9 (68 - 84)	
	PSN (10 nM)	7.2 ± 0.3	78.4 (55 - 102)	0.4 ± 15.0
	PSN (100 nM)	7.1 ± 0.1	66.3 (58 - 74)	11.0 ± 3.4
	PSN (1 µM)	6.8 ± 0.4	25.9 (13 - 39) †	65.0 ± 10.7

[a] Negative logarithm of the agonist EC_{50} value, determined using nonlinear regression analysis. Values represent the mean ± standard error of the mean (SEM) of 4-6 experiments.[b] Maximal agonist effect, determined using nonlinear regression analysis. Values represent the mean with 95% confidence limits (CL) of 4-6 experiments.

†Significantly different (non-overlapping confidence limits) from the DMSO vehicle control).

Molecular Pharmacology Fast Forward. Published on November 15, 2012 as DOI: 10.1124/mol.112.080879
This article has not been copyedited and formatted. The final version may differ from this version.

Table 2: **Effect of Org 27569 on CP55940 and WIN55212 in [^{35}S] GTPγS binding, cAMP and pERK assay in hCB1R cells**.

Agonist	Vehicle/modulator	pEC_{50} [a]	E_{max} [b] (%) (95% confidence limits)	% Inhibition ± S.E.M
[^{35}S] GTPγS binding (% stimulation above basal)				
CP55940	**DMSO**	7.3 ± 0.2	64.7 (57 - 72)	
	Org 27569 (10 nM)	6.2 ± 0.4	76.2 (48 - 105)	13.8 ± 31
	Org 27569 (100 nM)	6.9 ± 0.6	35.2 (19 - 52) †	46.3 ± 18
	Org 27569 (1 µM)	-	- †	94.4 ±6.0
WIN55212	**DMSO**	6.7 ± 0.2	70.4 (62 - 79)	
	Org 27569 (100 nM)	6.5 ± 0.3	67.7 (49 - 87)	1.2 ± 16
	Org 27569 (1 µM)	6.9 ± 0.4	33.1 (20 - 47) †	43.4 ± 18
cAMP Assay (% inhibition of forskolin stimulation)				
CP55940	**DMSO**	8.1 ± 0.2	86.6 (75 - 98)	
	Org 27569 (10 nM)	7.6 ± 0.4	55.0 (37 - 73) †	30.3 ± 12.0
	Org 27569 (100 nM)	-	-†	155 ± 9.6
WIN55212	**DMSO**	7.1 ± 0.2	78.6 (64 - 93)	
	Org 27569 (100 nM)	7.0 ± 0.2	64.6 (51 - 78)	22.3 ± 4.9
	Org 27569 (1 µM)	6.9 ± 0.3	41.1 (23 - 59) †	37.0 ± 5.9
ERK1/2 phosphorylation (% increase above basal)				
CP55940	**DMSO**	7.6 ± 0.14	50.0 (44 - 56)	
	Org 27569 (100 nM)	8.0 ± 0.16	72.0 (64 - 80) †	-
	Org 27569 (1 µM)	7.8 ± 0.23	65.0 (58 -72) †	-
WIN55212	**DMSO**	6.6 ± 0.53	40.2 (27 - 54)	
	Org 27569 (100 nM)	7.0 ± 0.67	50.9 (35 - 66)	-
	Org 27569 (1 µM)	6.6 ± 0.48	37.0 (24 - 51)	-

[a] Negative logarithm of the agonist EC_{50} value, determined using nonlinear regression analysis. Values represent the mean ± standard error of the mean (SEM) of 4-6 experiments.[b] Maximal agonist effect, determined using nonlinear regression analysis. Values represent the mean with 95% confidence limits (CL) of 4-6 experiments.†Significantly different (non-overlapping confidence limits) from the DMSO vehicle.

Molecular Pharmacology Fast Forward. Published on November 15, 2012 as DOI: 10.1124/mol.112.080879
This article has not been copyedited and formatted. The final version may differ from this version.

Table 3: **Effect of Org 27569 and PSNCBAM-1 on CP55940 and WIN55212-2 in the PathHunter® beta-arrestin assay.** Increase in luminescence (relative light units, RLU) are presented as a percentage of the maximal CP55940 stimulation.

.

Agonist	Vehicle/modulator	pEC_{50} [a]	E_{max} [b] (%) (95% CL)	% Inhibition ± S.E.M
CP55940	**DMSO**	7.9 ± 0.06	99.5 (95 - 104)	
	Org 27569 (1 nM)	8.1 ± 0.1	66.7 (60 - 73) †	32.9 ± 5.2
	Org 27569 (10 nM)	8.0 ± 0.1	15.3 (13.5 - 17) †	84.3 ± 1.1
	Org 27569 (100 nM)	-	-†	98.9 ± 0.2
WIN55212	**DMSO**	6.9 ± 0.1	83.5 (70 - 97)	
	Org 27569 (1 nM)	7.1 ± 0.07	76.4 (70 - 83)	8.5 ± 2.7
	Org 27569 (10 nM)	7.0 ± 0.1	37.9 (33 - 43) †	54.2 ± 0.7
	Org 27569 (100 nM)	7.3 ± 0.7	3.4 (0.3 - 7) †	94.6 ± 1.7
Anandamide	**DMSO**	7.4 ± 0.2	100.0 (83– 117)	
	Org 27569 (1 nM)	7.0 ± 0.1	110.9 (96 - 126)	-10.92 ± 0.6
	Org 27569 (10 nM)	6.0 ± 0.6	- †	80.2 ± 3.3
	Org 27569 (100 nM)	8.8 ± 1.6	- †	135 ± 1.8
CP55940	**DMSO**	7.9 ± 0.06	102.3 (98 - 107)	
	PSNCBAM (1 nM)	7.9 ± 0.1	76.8 (70 - 83) †	24.5 ± 4.3
	PSNCBAM (10 nM)	8.6 ± 0.3	18.3 (15 - 21) †	82.1 ± 1.2
	PSNCBAM (100 nM)	-	-†	96.9 ± 2.1
WIN55212	**DMSO**	7.6 ± 0.1	101.3 (90 - 112)	
	PSNCBAM (1 nM)	7.5 ± 0.1	90.2 (82 - 98)	10.0 ± 6.6
	PSNCBAM (10 nM)	7.8 ± 0.2	46.1 (39 - 53) †	53.8 ± 3.7
	PSNCBAM (100 nM)	8.6 ± 1.5	8.9 (5 - 13) †	90.5 ± 2.6

[a] Negative logarithm of the agonist EC_{50} value, determined using nonlinear regression analysis. Values represent the mean ± standard error of the mean (SEM) of 4-6 experiments.[b] Maximal agonist effect, determined using nonlinear regression analysis. Values represent the mean with 95% confidence limits (CL) of 4-6 experiments.†Significantly different (non-overlapping confidence limits) from the DMSO vehicle.

Molecular Pharmacology Fast Forward. Published on November 15, 2012 as DOI: 10.1124/mol.112.080879
This article has not been copyedited and formatted. The final version may differ from this version.

Table 4: Effect of allosteric modulators on saturation binding of [^{3}H]CP55940 in mouse brain membranes and hCB1 cell membranes. Data shown are mean with 95% confidence limits (CL) of 3 - 6 independent experiments.

	Kd(nM) (95% CL)	**Bmax (pmolmg^{-1}) (95% CL)**
Mouse Brain Membranes		
[^{3}H]CP55 + Vehicle	2.67 (1.5 - 3.8)	1.59 (1.3 - 1.8)
[^{3}H]CP55 + Org (1µM)	2.16 (1.5 - 2.8)	2.43 (2.2 - 2.7) †
[^{3}H]CP55 + Org (10µM)	2.76 (1.7 - 3.8)	3.25 (2.8 - 3.7) †
[^{3}H]CP55 + PSN (1µM)	6.00 (3.1 - 8.9)	3.64 (2.7 - 4.5) †
[^{3}H]CP55 + PSN (10µM)	5.66 (3.6 - 7.7)	2.98 (2.4 - 3.5) †
hCB$_1$		
[^{3}H]CP55 + Vehicle	0.45 (0.26 - 0.63)	6.4 (5.5 - 8.4)
[^{3}H]CP55 + PSN (1µM)	0.56 (0.45 - 0.66)	11 (10.8 - 12.2) †

Molecular Pharmacology Fast Forward. Published on November 15, 2012 as DOI: 10.1124/mol.112.080879
This article has not been copyedited and formatted. The final version may differ from this version.

Table 5: Effect of PSNCBAM-1 on [^{3}H]CP55940 (0.5nM) dissociation from hCB1 cell membranes. Data shown are mean ± SEM of 3 independent experiments. *, $P < 0.05$ **, $P < 0.01$ one-way ANOVA followed by Dunnett's multiple comparison

	Slow Phase (%)	**K_{off} (slow) ($min^{-1}x10^{-2}$)**	**K_{off} (fast) ($min^{-1}x10^{-2}$**
[^{3}H]CP55 +Vehicle	59.7 ± 1.9	1.1 ± 0.2	32 ± 20
[^{3}H]CP55 + 30nM PSN	64.4 ± 3.9	1.2 ± 0.1	63 ± 22
[^{3}H]CP55 + 100nM PSN	79.0 ± 4.0**	0.9 ± 0.1	34 ± 9
[^{3}H]CP55 + 2μM PSN	100 ± 0 **	0.4 ± 0.04*	-

Molecular Pharmacology Fast Forward. Published on November 15, 2012 as DOI: 10.1124/mol.112.080879
This article has not been copyedited and formatted. The final version may differ from this version.

Table 6 Effect of Gpp(NH)p and PSNCBAM-1 on [^{3}H]CP55940 dissociation from hCB1 cell membranes. Control data are mean ± SEM of 3 experiments. Data in the presence of Gpp(NH)p are mean with 95% confidence limits (CL) of 2 independent experiments.

	Slow Phase (%, 95% CL)	**K_{off} (slow) ($min^{-1}x10^{-2}$) (95% CL)**	**K_{off} (fast) ($min^{-1}x10^{-2}$) (%, 95% CL)**
Control	57.4 (54.6 – 59.8)	1.1 (0.7 – 1.7)	32 (8.9 – 111.5)
100μM Gpp(NH)p	29 (25 – 33) †	2.2 (2.4 – 2.1) †	44.3 (44.2 – 44.4)
100μM Gpp(NH)p + 2μM PSN	58 (57 – 59)	0.9 (0.8 – 1.0)	49.6 (47.1 – 52.2)

†Significantly different (non-overlapping confidence limits) from the DMSO vehicle.

Molecular Pharmacology Fast Forward. Published on November 15, 2012 as DOI: 10.1124/mol.112.080879
This article has not been copyedited and formatted. The final version may differ from this version.

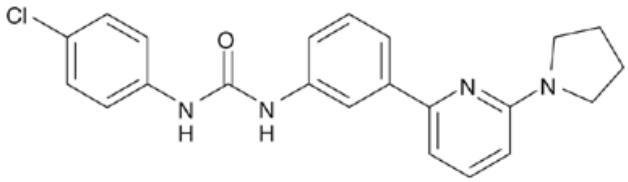

PSNCBAM-1

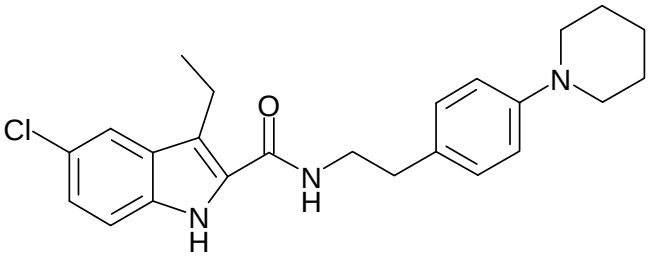

Org 27569

Fig 1

Molecular Pharmacology Fast Forward. Published on November 15, 2012 as DOI: 10.1124/mol.112.080879
This article has not been copyedited and formatted. The final version may differ from this version.

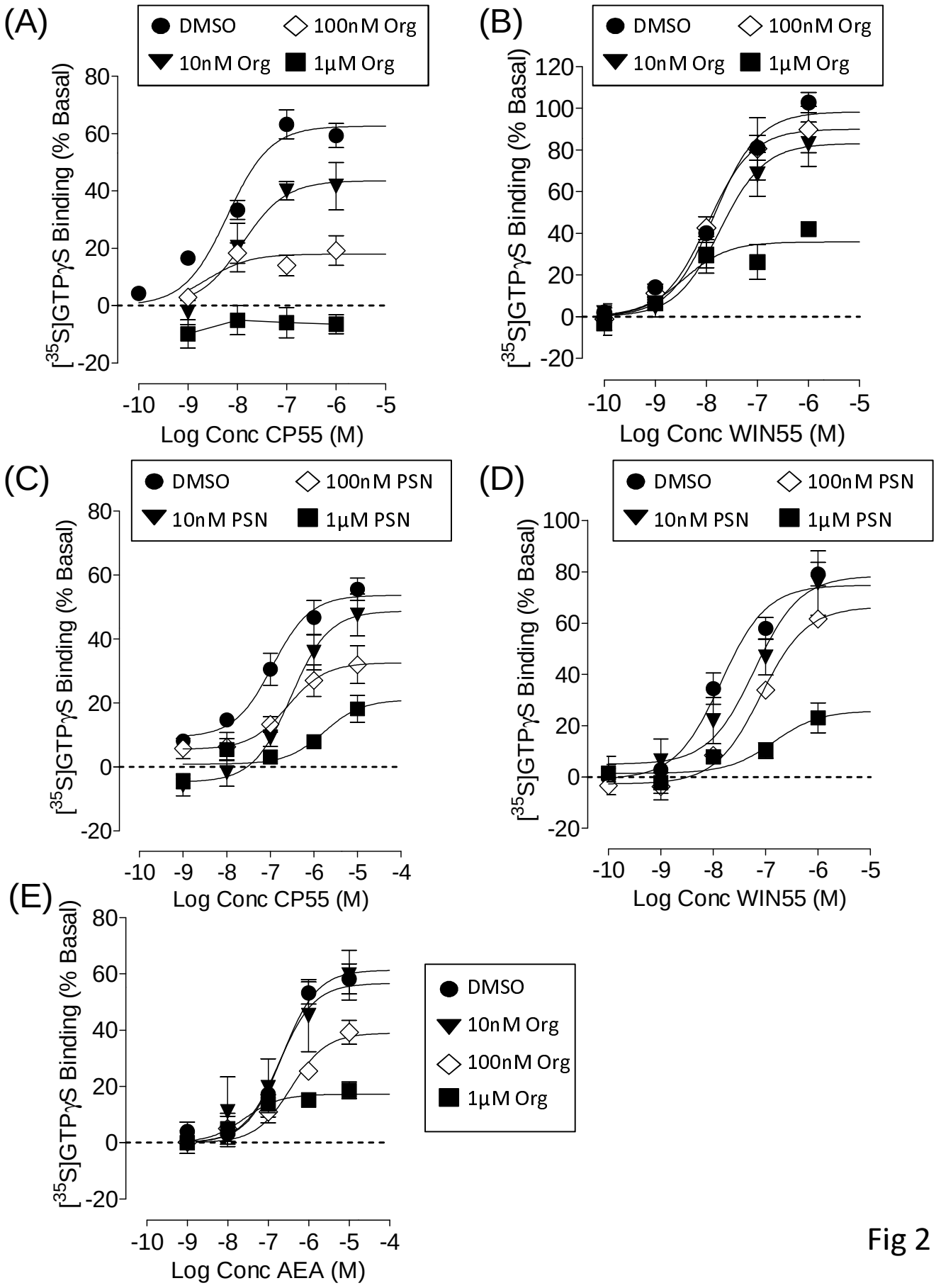

Fig 2

Molecular Pharmacology Fast Forward. Published on November 15, 2012 as DOI: 10.1124/mol.112.080879
This article has not been copyedited and formatted. The final version may differ from this version.

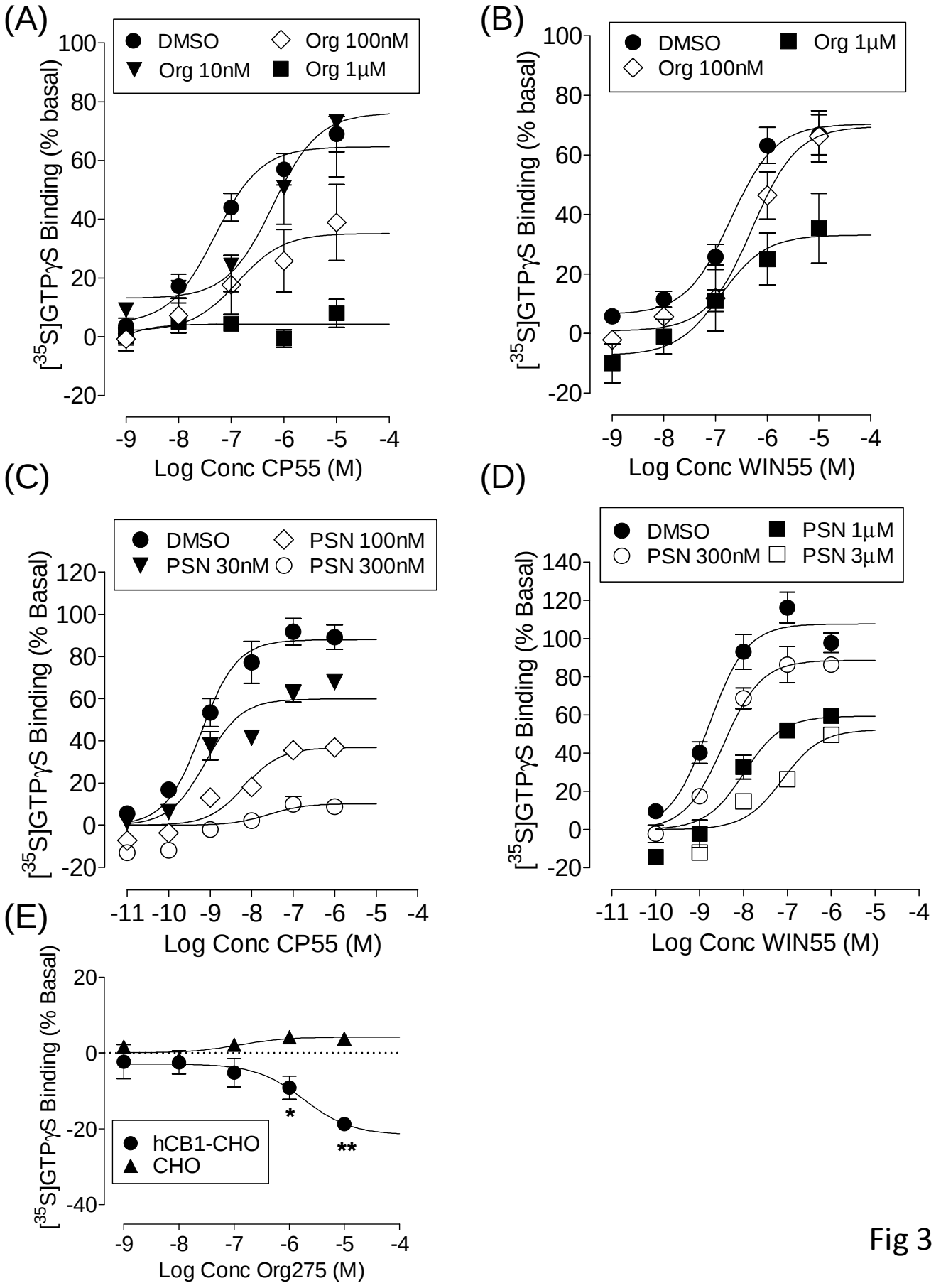

Fig 3

Molecular Pharmacology Fast Forward. Published on November 15, 2012 as DOI: 10.1124/mol.112.080879
This article has not been copyedited and formatted. The final version may differ from this version.

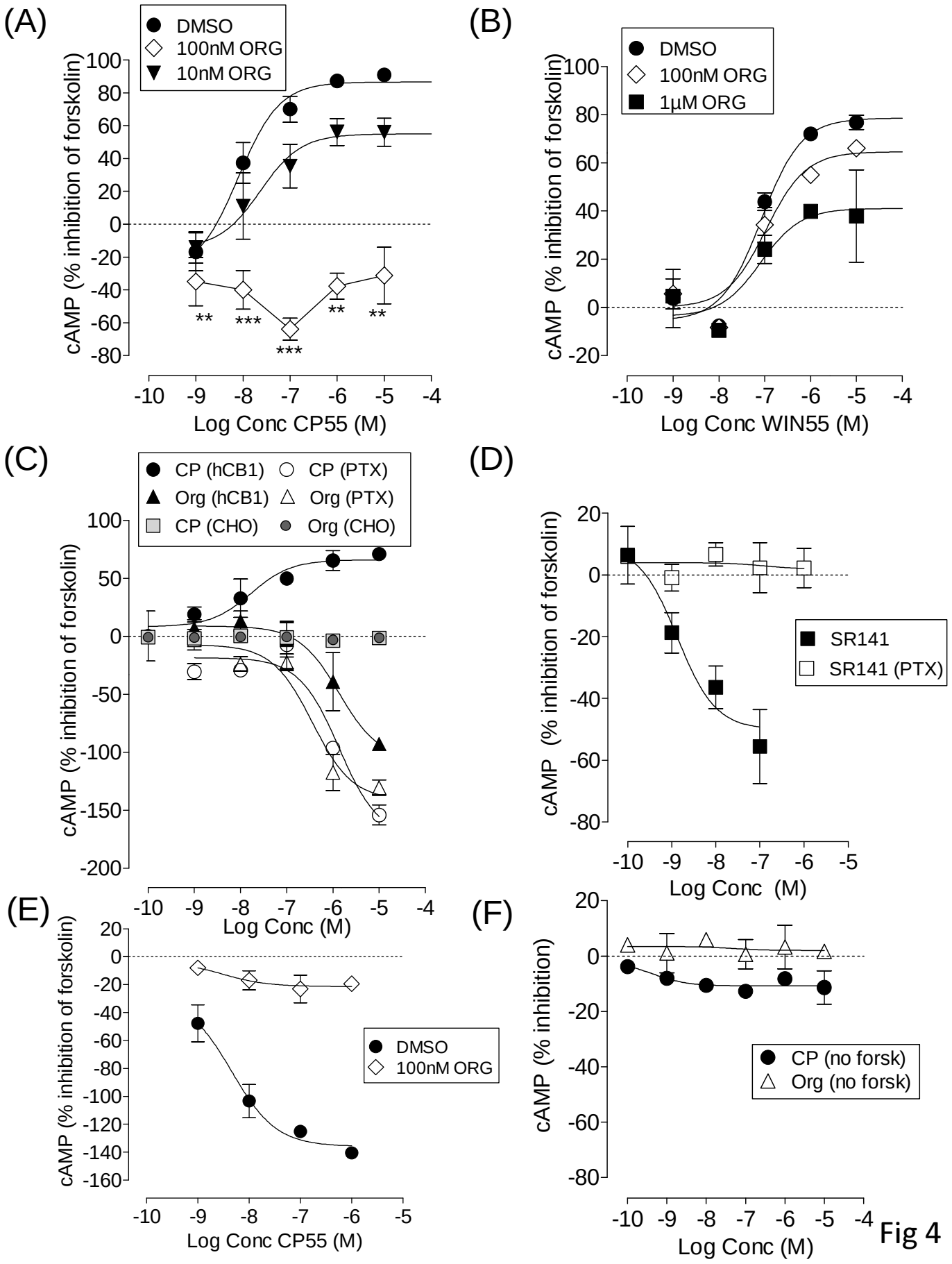

Fig 4

Molecular Pharmacology Fast Forward. Published on November 15, 2012 as DOI: 10.1124/mol.112.080879
This article has not been copyedited and formatted. The final version may differ from this version.

Fig 5

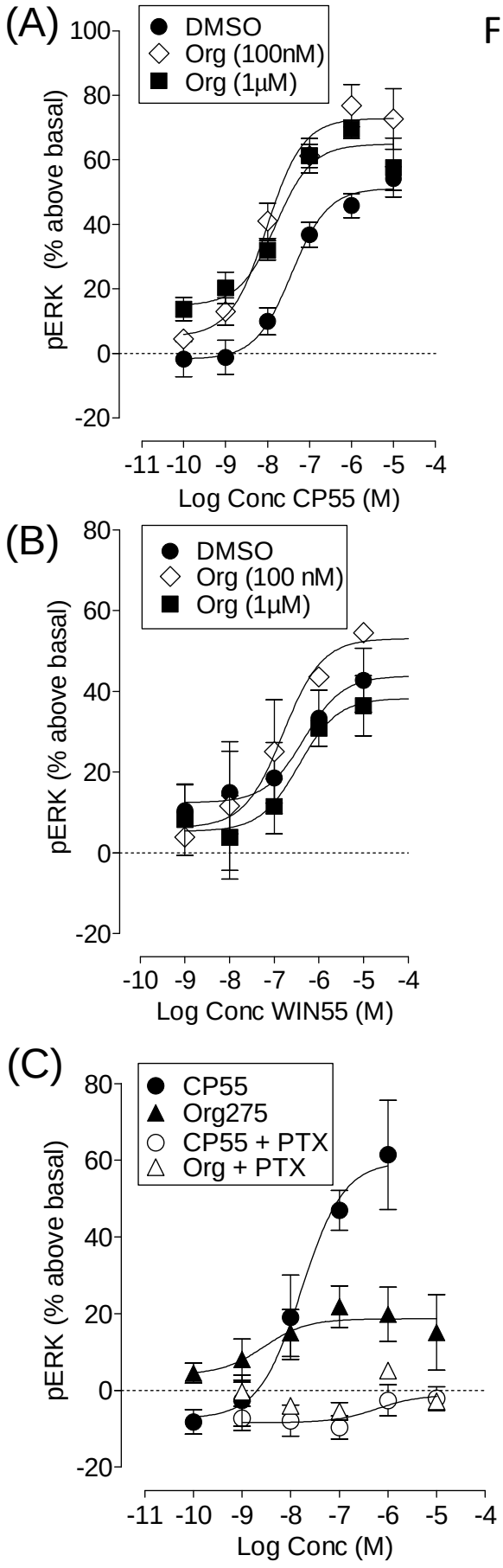

Molecular Pharmacology Fast Forward. Published on November 15, 2012 as DOI: 10.1124/mol.112.080879
This article has not been copyedited and formatted. The final version may differ from this version.

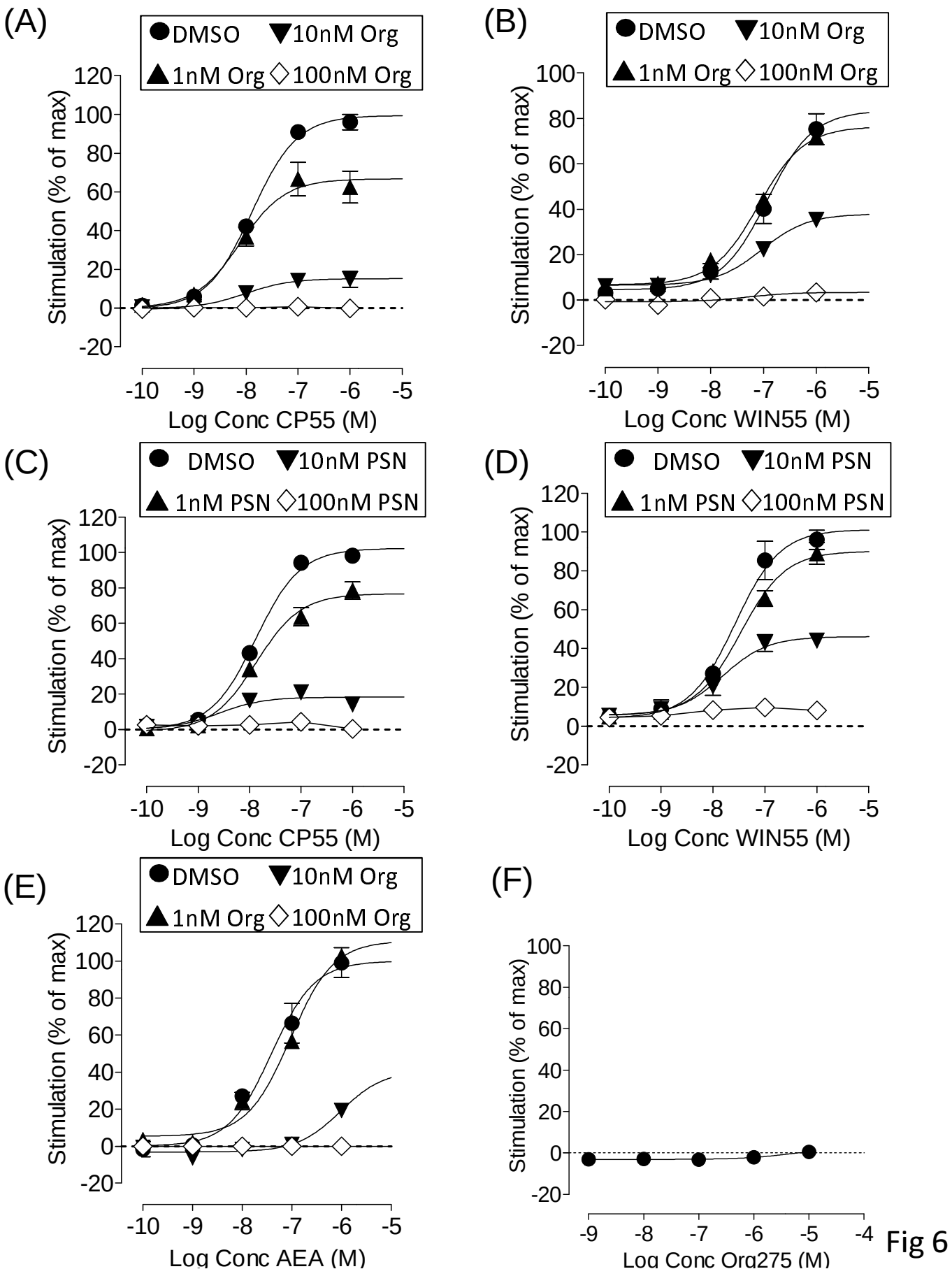

Fig 6

Molecular Pharmacology Fast Forward. Published on November 15, 2012 as DOI: 10.1124/mol.112.080879
This article has not been copyedited and formatted. The final version may differ from this version.

Fig 7

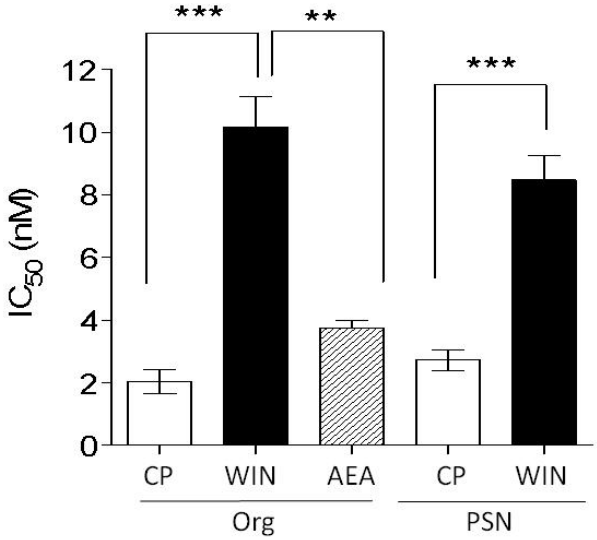

Molecular Pharmacology Fast Forward. Published on November 15, 2012 as DOI: 10.1124/mol.112.080879
This article has not been copyedited and formatted. The final version may differ from this version.

Fig 8

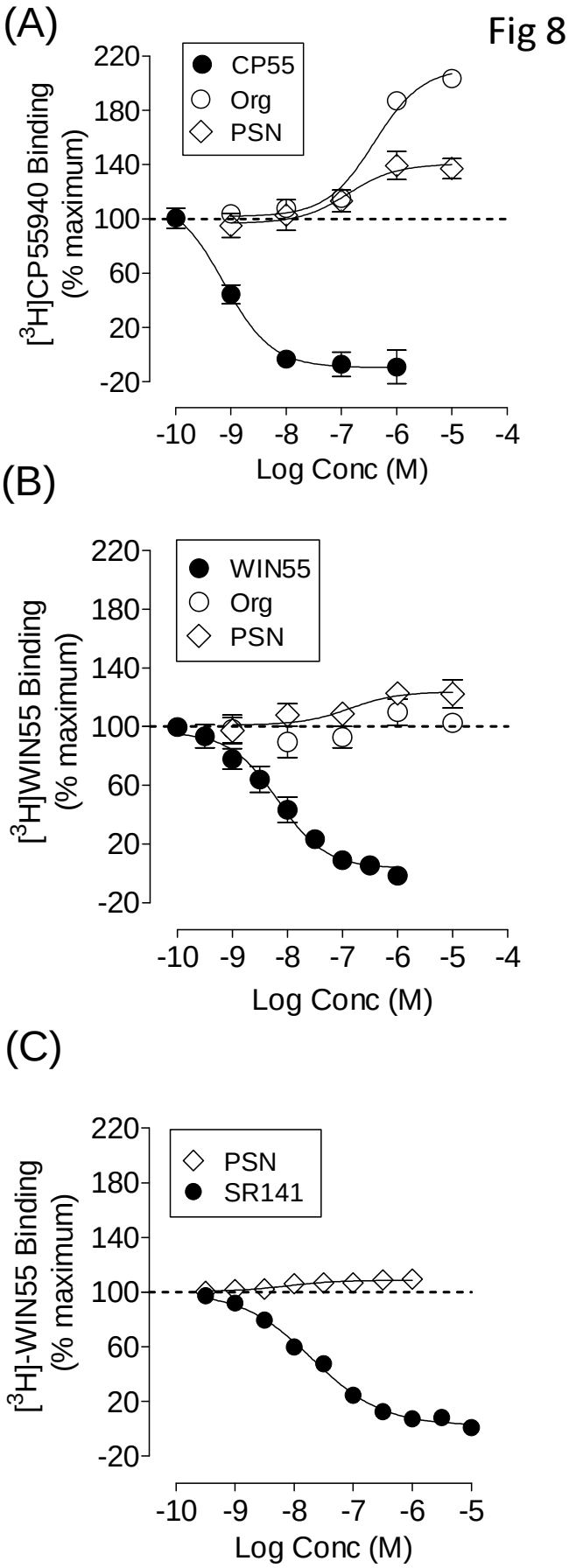

Molecular Pharmacology Fast Forward. Published on November 15, 2012 as DOI: 10.1124/mol.112.080879
This article has not been copyedited and formatted. The final version may differ from this version.

Fig 9

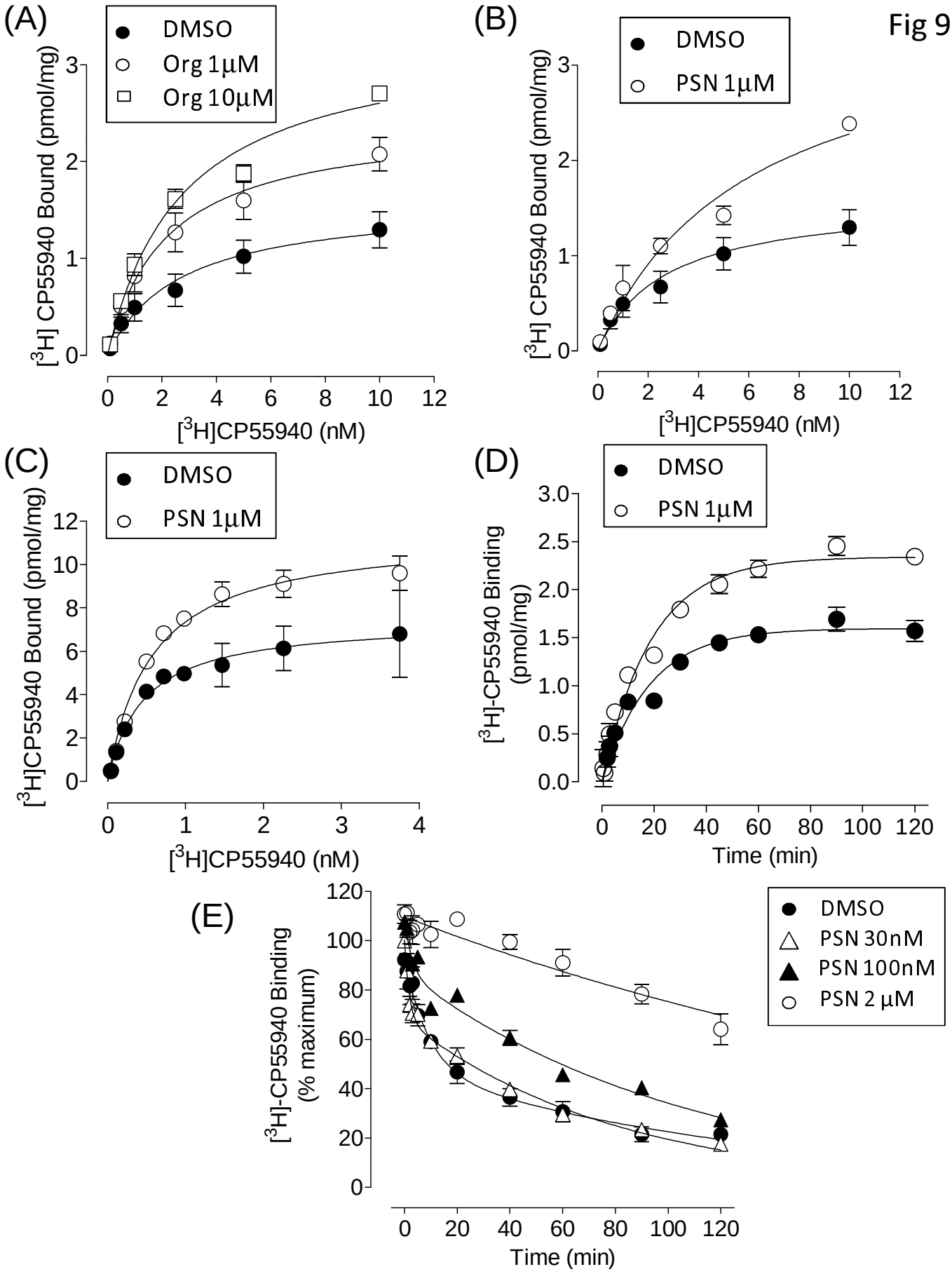

Molecular Pharmacology Fast Forward. Published on November 15, 2012 as DOI: 10.1124/mol.112.080879
This article has not been copyedited and formatted. The final version may differ from this version.

Fig 10

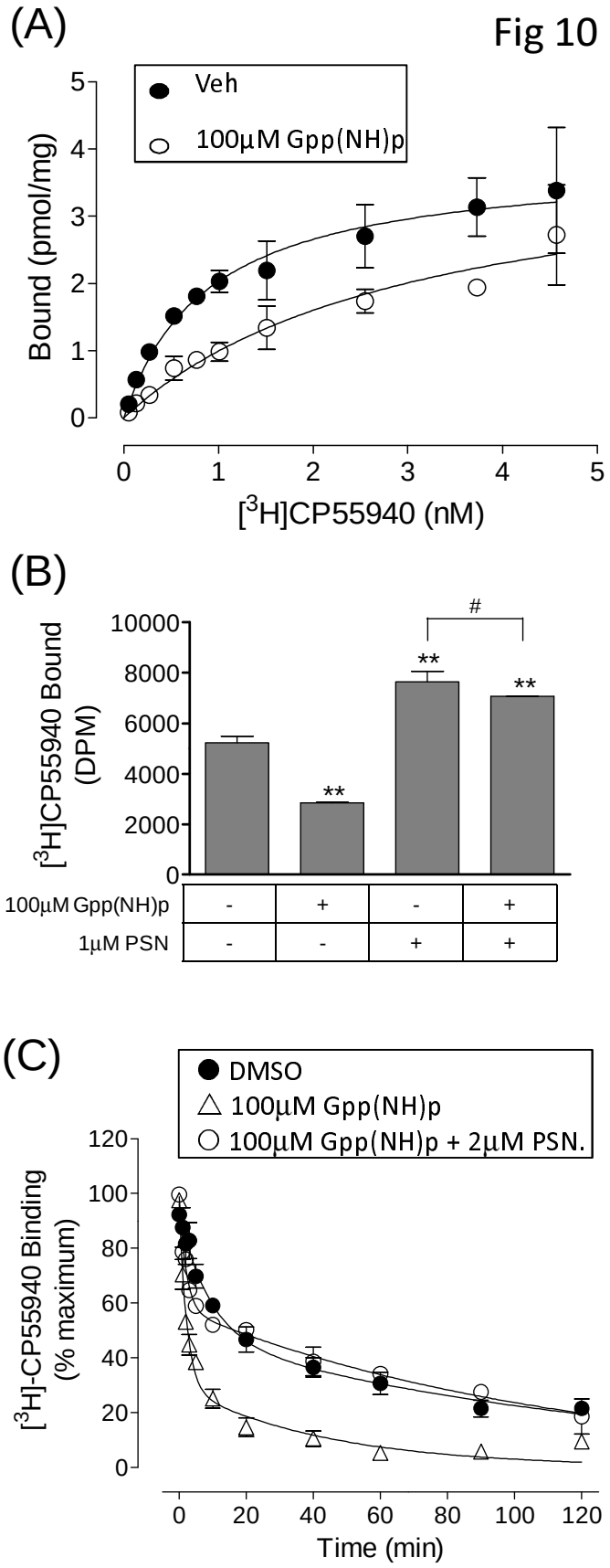

Molecular Pharmacology Fast Forward. Published on November 15, 2012 as DOI: 10.1124/mol.112.080879
This article has not been copyedited and formatted. The final version may differ from this version.

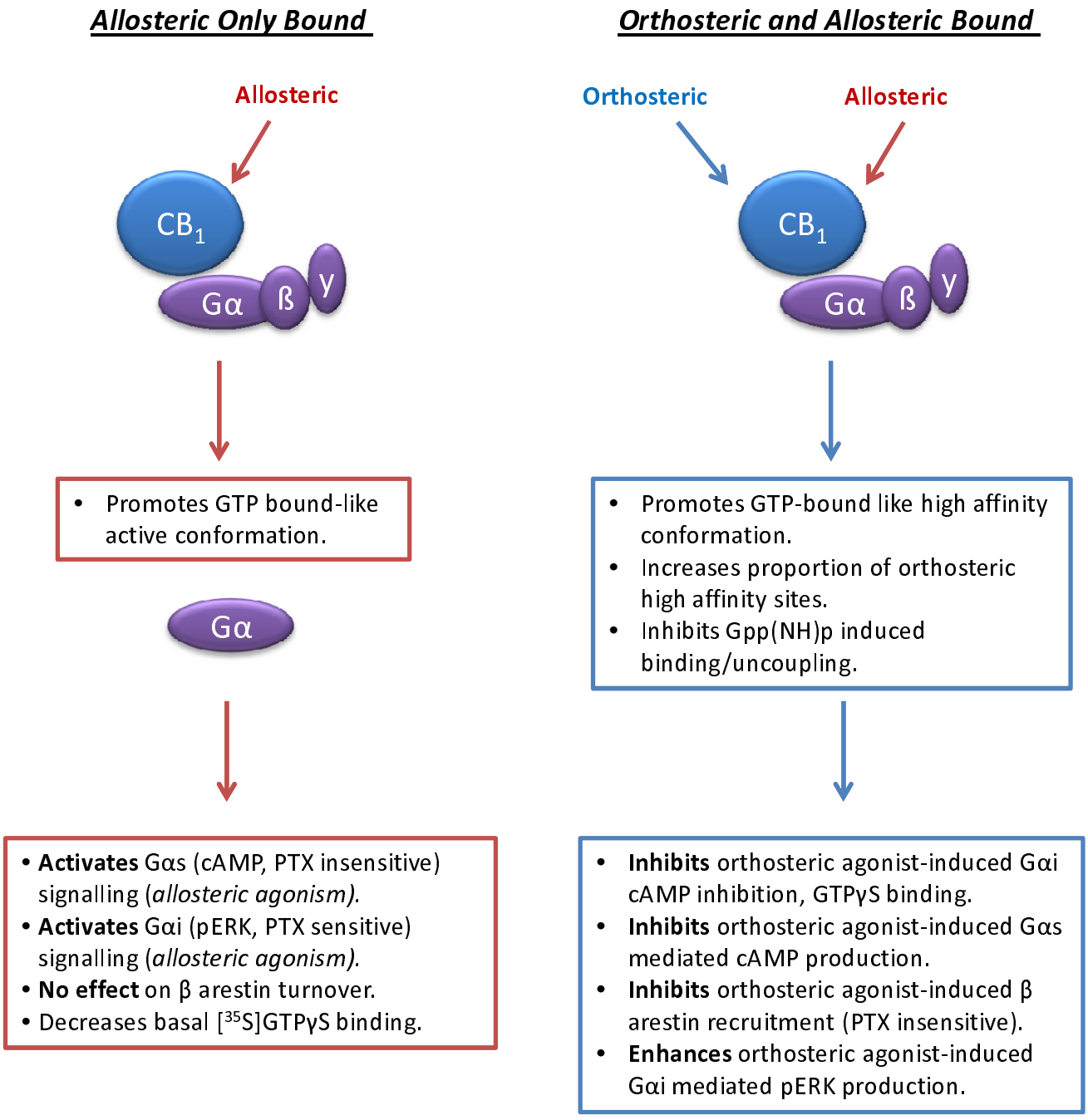

Fig 11